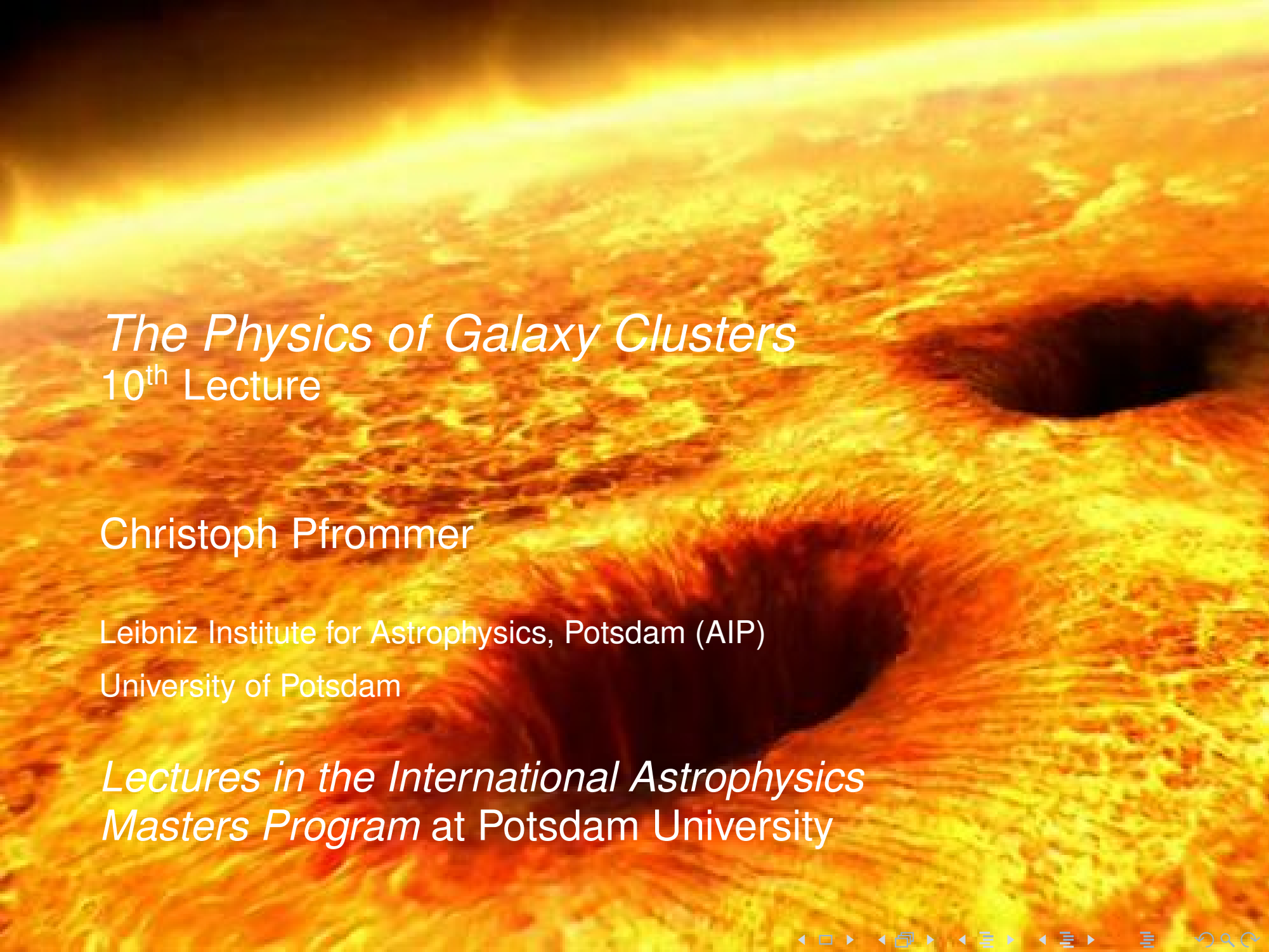

The Physics of Galaxy Clusters
10th Lecture

Christoph Pfrommer

Leibniz Institute for Astrophysics, Potsdam (AIP)

University of Potsdam

Lectures in the International Astrophysics Masters Program at Potsdam University

- **Radiative cooling**
  * Thermal bremsstrahlung emission main cooling mechanism in massive clusters
  * Cooling fastest in the cluster centers
  * Cool core (CC) cluster: central cooling time $t_{\mathrm{cool}} < 1$ Gyr and central entropy $K_0 < 30$ keV cm^2
  * Non-cool core (NCC) clusters have no severe overcooling problem

- **Radiative cooling**
  * Thermal bremsstrahlung emission main cooling mechanism in massive clusters
  * Cooling fastest in the cluster centers
  * Cool core (CC) cluster: central cooling time $t_{\mathrm{cool}} < 1$ Gyr and central entropy $K_0 < 30$ keV cm^2
  * Non-cool core (NCC) clusters have no severe overcooling problem
- **Supernova feedback**
  * Supernova feedback not energetic enough to balance cooling rates
  * radiative losses of ICM are too strong to solve the "cooling flow problem"

- **Radiative cooling**
  * Thermal bremsstrahlung emission main cooling mechanism in massive clusters
  * Cooling fastest in the cluster centers
  * Cool core (CC) cluster: central cooling time $t_{\mathrm{cool}} < 1$ Gyr and central entropy $K_0 < 30$ keV cm^2
  * Non-cool core (NCC) clusters have no severe overcooling problem
- **Supernova feedback**
  * Supernova feedback not energetic enough to balance cooling rates
  * radiative losses of ICM are too strong to solve the "cooling flow problem"
- **AGN jet feedback**
  * promising mechanisms for self-regulated feedback
  * energetics and heating rate sufficient for balancing cooling losses, but not for transforming CC to NCC clusters
  * many open questions regarding the specific heating mechanism and tuning of self-regulation across 8 orders of magnitude

Heat conduction – 1

- A system can be in hydrostatic equilibrium, but out of thermal equilibrium. In the absence of viscosity, the entropy equation for smooth, differentiable flows reads

$$\rho T \frac{\mathrm{d}s}{\mathrm{d}t} = \boldsymbol{\nabla} \cdot (\kappa \boldsymbol{\nabla} T) \,. \tag{1}$$

Using $\mathrm{d}q = T\mathrm{d}s$ and $c_P \equiv (\mathrm{d}q/\mathrm{d}T)_P$, we get

$$c_P \mathrm{d}T = T\mathrm{d}s \quad \Rightarrow \quad \mathrm{d}s = c_P \mathrm{d}\ln T.$$

Heat conduction – 1

- A system can be in hydrostatic equilibrium, but out of thermal equilibrium. In the absence of viscosity, the entropy equation for smooth, differentiable flows reads

$$\rho T \frac{\mathrm{d}s}{\mathrm{d}t} = \boldsymbol{\nabla} \cdot (\kappa \boldsymbol{\nabla} T) \,. \tag{1}$$

  Using $\mathrm{d}q = T\mathrm{d}s$ and $c_P \equiv (\mathrm{d}q/\mathrm{d}T)_P$, we get

$$c_P \mathrm{d}T = T\mathrm{d}s \quad \Rightarrow \quad \mathrm{d}s = c_P \mathrm{d}\ln T.$$

- Hence, we can rewrite Eqn. (1) while assuming $\kappa = \text{const.}$,

$$\rho c_P \frac{\mathrm{d}T}{\mathrm{d}t} = \kappa \boldsymbol{\nabla}^2 T \quad \text{or} \quad \frac{\mathrm{d}T}{\mathrm{d}t} = \chi \boldsymbol{\nabla}^2 T,$$

  where $\chi \equiv \kappa/(\rho c_P)$. This shows that the temperature of a smooth flow can only change as a result of thermal conduction if $\boldsymbol{\nabla} T \neq \mathbf{0}$ since the temperature gradient is the source of free energy.
- We now want to estimate the heat conductivity κ.

Heat conduction – 2

- To estimate κ, we consider a system in thermal equilibrium with a temperature T and with particles moving randomly in all directions. ΔA denotes the area of a screen perpendicular to the x axis. The number of particles that fly per unit time with an *rms* velocity v through the screen from one side to the other is given by

$$\frac{\Delta N}{\Delta t} = \frac{nv\Delta A}{6},$$

where the factor of 6 arises because on average, 1/3 of all particles fly along the x axis and of those, only 1/2 in either direction.

Heat conduction – 2

- To estimate κ, we consider a system in thermal equilibrium with a temperature T and with particles moving randomly in all directions. ΔA denotes the area of a screen perpendicular to the x axis. The number of particles that fly per unit time with an *rms* velocity v through the screen from one side to the other is given by

$$\frac{\Delta N}{\Delta t} = \frac{nv\Delta A}{6},$$

  where the factor of 6 arises because on average, 1/3 of all particles fly along the x axis and of those, only 1/2 in either direction.

- The particle mean free path is $\lambda_{\rm mfp} = 1/(n\sigma)$ where σ is the collisional cross section. Particles at $x - \lambda_{\rm mfp}$ transport gas properties to x and vice versa. This is particularly important for gradients in gas properties that will be smoothed out as a result of such a transport.

Heat conduction – 2

- To estimate κ, we consider a system in thermal equilibrium with a temperature T and with particles moving randomly in all directions. ΔA denotes the area of a screen perpendicular to the x axis. The number of particles that fly per unit time with an *rms* velocity v through the screen from one side to the other is given by

$$\frac{\Delta N}{\Delta t} = \frac{nv\Delta A}{6},$$

  where the factor of 6 arises because on average, 1/3 of all particles fly along the x axis and of those, only 1/2 in either direction.

- The particle mean free path is $\lambda_{\rm mfp} = 1/(n\sigma)$ where σ is the collisional cross section. Particles at $x - \lambda_{\rm mfp}$ transport gas properties to x and vice versa. This is particularly important for gradients in gas properties that will be smoothed out as a result of such a transport.

- Hence, in the presence of a density gradient, $\partial n/\partial x \neq 0$, the net number of particles flying from the denser to the more dilute region is

$$\frac{\Delta N}{\Delta t} = \frac{n(x+\lambda_{\rm mfp})v\Delta A}{6} - \frac{n(x-\lambda_{\rm mfp})v\Delta A}{6} \approx \frac{v\Delta A}{6}\frac{\partial n}{\partial x}2\lambda_{\rm mfp},$$

  where we have expanded the density field to first order and have assumed that the typical length of a gradient Δx is much larger than the mean free path, $\lambda_{\rm mfp} \ll \Delta x$.

Heat conduction – 3

- The diffusion coefficient that relates the particle current $j = \Delta N/(\Delta t \Delta A)$ to the number density gradient is given by

$$\frac{\Delta N}{\Delta t \Delta A} \stackrel{!}{=} D\frac{\partial n}{\partial x} \quad \text{where} \quad D \equiv \frac{v\lambda_{\mathrm{mfp}}}{3} = \frac{v}{3n\sigma}.$$

Heat conduction – 3

- The diffusion coefficient that relates the particle current $j = \Delta N/(\Delta t \Delta A)$ to the number density gradient is given by

$$\frac{\Delta N}{\Delta t \Delta A} \stackrel{!}{=} D\frac{\partial n}{\partial x} \quad \text{where} \quad D \equiv \frac{v\lambda_{\mathrm{mfp}}}{3} = \frac{v}{3n\sigma}.$$

- If the temperature changes along x (i.e., $\partial T/\partial x \neq 0$), the particles transport energy,

$$\begin{aligned}\frac{\Delta E}{\Delta t \Delta A} &= \frac{nv}{6}[E(x+\lambda_{\mathrm{mfp}}) - E(x-\lambda_{\mathrm{mfp}})] \\ &= \frac{nv\lambda_{\mathrm{mfp}}}{3}\left(\frac{\partial E}{\partial T}\frac{\partial T}{\partial x}\right) = \frac{nvc_V\lambda_{\mathrm{mfp}}}{3}\frac{\partial T}{\partial x},\end{aligned}$$

where c_V is the heat capacity at constant volume. Hence, we find

$$\frac{\Delta E}{\Delta t \Delta A} \stackrel{!}{=} \kappa\frac{\partial T}{\partial x} \quad \text{where} \quad \kappa = \frac{nvc_V\lambda_{\mathrm{mfp}}}{3} = \frac{vc_V}{3\sigma} = \frac{vk_{\mathrm{B}}}{2\sigma},$$

where we used the heat capacity at constant volume $c_V = 3k_{\mathrm{B}}/2$ in the last step (assuming an ideal, monoatomic gas) and the heat conductivity κ has units of erg cm^{-1} s^{-1} K^{-1}.

Heat conduction – 3

- The diffusion coefficient that relates the particle current $j = \Delta N/(\Delta t \Delta A)$ to the number density gradient is given by

$$\frac{\Delta N}{\Delta t \Delta A} \stackrel{!}{=} D\frac{\partial n}{\partial x} \quad \text{where} \quad D \equiv \frac{v\lambda_{\mathrm{mfp}}}{3} = \frac{v}{3n\sigma}.$$

- If the temperature changes along x (i.e., $\partial T/\partial x \neq 0$), the particles transport energy,

$$\begin{aligned}\frac{\Delta E}{\Delta t \Delta A} &= \frac{nv}{6}[E(x+\lambda_{\mathrm{mfp}}) - E(x-\lambda_{\mathrm{mfp}})] \\ &= \frac{nv\lambda_{\mathrm{mfp}}}{3}\left(\frac{\partial E}{\partial T}\frac{\partial T}{\partial x}\right) = \frac{nvc_V\lambda_{\mathrm{mfp}}}{3}\frac{\partial T}{\partial x},\end{aligned}$$

  where c_V is the heat capacity at constant volume. Hence, we find

$$\frac{\Delta E}{\Delta t \Delta A} \stackrel{!}{=} \kappa\frac{\partial T}{\partial x} \quad \text{where} \quad \kappa = \frac{nvc_V\lambda_{\mathrm{mfp}}}{3} = \frac{vc_V}{3\sigma} = \frac{vk_{\mathrm{B}}}{2\sigma},$$

  where we used the heat capacity at constant volume $c_V = 3k_{\mathrm{B}}/2$ in the last step (assuming an ideal, monoatomic gas) and the heat conductivity κ has units of erg cm^{-1} s^{-1} K^{-1}.
- Heat is conducted by electrons since they move faster than ions by $v_{\mathrm{e}}/v_{\mathrm{i}} = \sqrt{m_{\mathrm{i}}/m_{\mathrm{e}}} \approx 43\sqrt{Z}$ (assuming $T_{\mathrm{e}} = T_{\mathrm{i}}$ which applies to the ICM except for immediate post-shock regions). The electron mean free path is determined by the ion number density and the scattering cross section, implying $\lambda_{\mathrm{mfp}} = 1/(n_{\mathrm{i}}\sigma)$. Protons transport momentum and mediate viscosity.

Coulomb logarithm – 1

Electron scattering in the Coulomb field of an ion

- If the deflection angle is small, $\theta_\mathrm{D} \ll 1$, we can approximate θ_D by computing the perpendicular impulse exerted by the ion's Coulomb field, integrating along the electron's unperturbed straight line trajectory (the "Born approximation")

$$
\begin{aligned}
m_\mathrm{e} v_\mathrm{e} \theta_\mathrm{D} &= \int_{-\infty}^{\infty} \boldsymbol{e}_\perp \cdot \boldsymbol{\nabla}_\perp \phi_i \mathrm{d}t = \int_{-\infty}^{\infty} \frac{\partial}{\partial b} \left(\frac{Ze^2}{\sqrt{b^2 + v_\mathrm{e}^2 t^2}} \right) \mathrm{d}t \\
&= \int_{-\infty}^{\infty} \frac{Ze^2 b \mathrm{d}t}{\left(b^2 + v_\mathrm{e}^2 t^2\right)^{3/2}} = \frac{Ze^2}{v_\mathrm{e}} \int_{-\infty}^{\infty} \frac{b^2 \mathrm{d}x}{b^3 (1 + x^2)^{3/2}} \\
&= \frac{Ze^2}{v_\mathrm{e} b} \left. \frac{x}{\sqrt{1 + x^2}} \right|_{-\infty}^{\infty} = \frac{2Ze^2}{b v_\mathrm{e}},
\end{aligned}
$$

where we substituted $x = v_\mathrm{e} t / b$ and b is the impact parameter of the electron's trajectory. Hence we obtain

$$
\theta_\mathrm{D} = \frac{b_0}{b} \quad \text{for} \quad b \gg b_0 \equiv \frac{2Ze^2}{m_\mathrm{e} v_\mathrm{e}^2}.
$$

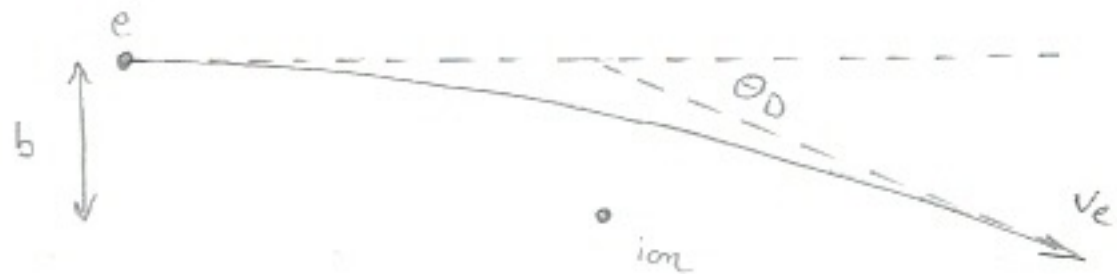

Coulomb logarithm – 1

Electron scattering in the Coulomb field of an ion

- If the deflection angle is small, $\theta_\mathrm{D} \ll 1$, we can approximate θ_D by computing the perpendicular impulse exerted by the ion's Coulomb field, integrating along the electron's unperturbed straight line trajectory (the "Born approximation")

$$m_\mathrm{e} v_\mathrm{e} \theta_\mathrm{D} = \int_{-\infty}^{\infty} \boldsymbol{e}_\perp \cdot \boldsymbol{\nabla}_\perp \phi_i \mathrm{d}t = \int_{-\infty}^{\infty} \frac{\partial}{\partial b} \left(\frac{Ze^2}{\sqrt{b^2 + v_\mathrm{e}^2 t^2}} \right) \mathrm{d}t$$

$$= \int_{-\infty}^{\infty} \frac{Ze^2 b \mathrm{d}t}{\left(b^2 + v_\mathrm{e}^2 t^2\right)^{3/2}} = \frac{Ze^2}{v_\mathrm{e}} \int_{-\infty}^{\infty} \frac{b^2 \mathrm{d}x}{b^3 (1+x^2)^{3/2}}$$

$$= \frac{Ze^2}{v_\mathrm{e} b} \left. \frac{x}{\sqrt{1+x^2}} \right|_{-\infty}^{\infty} = \frac{2Ze^2}{b v_\mathrm{e}},$$

where we substituted $x = v_\mathrm{e} t / b$ and b is the impact parameter of the electron's trajectory. Hence we obtain

$$\theta_\mathrm{D} = \frac{b_0}{b} \quad \text{for} \quad b \gg b_0 \equiv \frac{2Ze^2}{m_\mathrm{e} v_\mathrm{e}^2}.$$

- If the dominant source of this electron deflection were a single large-angle scattering event in the Coulomb field of an ion, then the relevant cross section would be $\sigma = \pi b_0^2$ (since all impact parameters $\lesssim b_0$ produce large-angle scatterings) and the mean deflection frequency ν_D and time t_D would be

$$\nu_\mathrm{D} = t_\mathrm{D}^{-1} = n_\mathrm{i} \sigma v_\mathrm{e} = n_\mathrm{i} \pi b_0^2 v_\mathrm{e} \quad \text{(for large-angle scattering)}. \tag{2}$$

Coulomb logarithm – 2

- The cumulative, random-walk effects of many small-angle electron scatterings off ions produce a net deflection of order a radian in a shorter time. As the directions of the individual scatterings are random, the mean defection angle after many scatterings vanish, $\langle\theta\rangle = 0$. However, $\langle\theta^2\rangle$ will not vanish and we have

$$\langle\theta^2\rangle = \sum_{\text{all encounters}} \theta_{\mathrm{D}}^2 = \sum_{\text{all encounters}} \left(\frac{b_0}{b}\right)^2 .$$

Coulomb logarithm – 2

- The cumulative, random-walk effects of many small-angle electron scatterings off ions produce a net deflection of order a radian in a shorter time. As the directions of the individual scatterings are random, the mean defection angle after many scatterings vanish, $\langle\theta\rangle = 0$. However, $\langle\theta^2\rangle$ will not vanish and we have

$$\langle\theta^2\rangle = \sum_{\text{all encounters}} \theta_{\mathrm{D}}^2 = \sum_{\text{all encounters}} \left(\frac{b_0}{b}\right)^2 .$$

- The number of encounters that occur with impact parameters between b and $b + \mathrm{d}b$ during time t is $\mathrm{d}N = n_{\mathrm{i}} v_{\mathrm{e}} t 2\pi b \mathrm{d}b$. Hence the mean square deflection angle accumulates up to

$$\langle\theta^2\rangle = \int_{b_{\min}}^{b_{\max}} \left(\frac{b_0}{b}\right)^2 \mathrm{d}N = n_{\mathrm{i}} 2\pi b_0^2 v_{\mathrm{e}} t \ln\left(\frac{b_{\max}}{b_{\min}}\right) .$$

Coulomb logarithm – 2

- The cumulative, random-walk effects of many small-angle electron scatterings off ions produce a net deflection of order a radian in a shorter time. As the directions of the individual scatterings are random, the mean defection angle after many scatterings vanish, $\langle\theta\rangle = 0$. However, $\langle\theta^2\rangle$ will not vanish and we have

$$\langle\theta^2\rangle = \sum_{\text{all encounters}} \theta_\mathrm{D}^2 = \sum_{\text{all encounters}} \left(\frac{b_0}{b}\right)^2 .$$

- The number of encounters that occur with impact parameters between b and $b + \mathrm{d}b$ during time t is $\mathrm{d}N = n_\mathrm{i} v_\mathrm{e} t 2\pi b \mathrm{d}b$. Hence the mean square deflection angle accumulates up to

$$\langle\theta^2\rangle = \int_{b_\mathrm{min}}^{b_\mathrm{max}} \left(\frac{b_0}{b}\right)^2 \mathrm{d}N = n_\mathrm{i} 2\pi b_0^2 v_\mathrm{e} t \ln\left(\frac{b_\mathrm{max}}{b_\mathrm{min}}\right) .$$

- While the integral diverges logarithmically, physics regularizes it quite naturally. The minimum impact parameter,

$$b_\mathrm{min} = \frac{Ze^2}{k_\mathrm{B} T},$$

equals the radius where the Coulomb energy of the electron in the field of the ion vanishes, $E = mv_\mathrm{e}^2/2 - Ze^2/b_\mathrm{min} \stackrel{!}{=} 0$.

Coulomb logarithm – 3

- The maximum impact parameter is given by the maximum distance over which electric fields of individual particles can reach without being screened by the oppositely charged particles in a plasma. This is known as the Debye length,

$$b_{\mathrm{max}} = \lambda_{\mathrm{D}} = \sqrt{\frac{k_{\mathrm{B}} T}{4\pi n_{\mathrm{e}} Z e^2}}.$$

Coulomb logarithm – 3

- The maximum impact parameter is given by the maximum distance over which electric fields of individual particles can reach without being screened by the oppositely charged particles in a plasma. This is known as the Debye length,

$$b_{\mathrm{max}} = \lambda_{\mathrm{D}} = \sqrt{\frac{k_{\mathrm{B}} T}{4\pi n_{\mathrm{e}} Z e^2}}.$$

- Hence, we can define the Coulomb logarithm

$$\begin{aligned}\ln \Lambda = \ln\left(\frac{b_{\mathrm{max}}}{b_{\mathrm{min}}}\right) &= \ln \sqrt{\frac{(k_{\mathrm{B}} T)^3}{4\pi n_{\mathrm{e}} Z^3 e^6}} \\ &= 35 - \frac{1}{2}\ln\left(\frac{n_{\mathrm{e}}}{10^{-2}\mathrm{cm}^{-3}}\right) + \frac{3}{2}\ln\left(\frac{k_{\mathrm{B}} T}{\mathrm{keV}}\right).\end{aligned}$$

Coulomb logarithm – 3

- The maximum impact parameter is given by the maximum distance over which electric fields of individual particles can reach without being screened by the oppositely charged particles in a plasma. This is known as the Debye length,

$$b_{\max} = \lambda_{\mathrm{D}} = \sqrt{\frac{k_{\mathrm{B}} T}{4\pi n_{\mathrm{e}} Z e^2}}.$$

- Hence, we can define the Coulomb logarithm

$$\begin{aligned}\ln\Lambda = \ln\left(\frac{b_{\max}}{b_{\min}}\right) &= \ln\sqrt{\frac{(k_{\mathrm{B}}T)^3}{4\pi n_{\mathrm{e}} Z^3 e^6}} \\ &= 35 - \frac{1}{2}\ln\left(\frac{n_{\mathrm{e}}}{10^{-2}\mathrm{cm}^{-3}}\right) + \frac{3}{2}\ln\left(\frac{k_{\mathrm{B}}T}{\mathrm{keV}}\right).\end{aligned}$$

- The value of t that implies $\langle\theta^2\rangle \approx 1$ is the deflection time t_{D},

$$\nu_{\mathrm{D}}^{\mathrm{ei}} = \frac{1}{t_{\mathrm{D}}^{\mathrm{ei}}} = n_{\mathrm{i}} 2\pi b_0^2 v_{\mathrm{e}} \ln\Lambda = \frac{8\pi n_{\mathrm{i}} Z^2 e^4}{m_{\mathrm{e}}^2 v_{\mathrm{e}}^3} \ln\Lambda \tag{3}$$

and $\ln\Lambda \approx 35 \ldots 40$ in the ICM.

Coulomb logarithm – 3

- The maximum impact parameter is given by the maximum distance over which electric fields of individual particles can reach without being screened by the oppositely charged particles in a plasma. This is known as the Debye length,

$$b_{\max} = \lambda_{\mathrm{D}} = \sqrt{\frac{k_{\mathrm{B}} T}{4\pi n_{\mathrm{e}} Z e^2}}.$$

- Hence, we can define the Coulomb logarithm

$$\begin{aligned}\ln\Lambda = \ln\left(\frac{b_{\max}}{b_{\min}}\right) &= \ln\sqrt{\frac{(k_{\mathrm{B}}T)^3}{4\pi n_{\mathrm{e}} Z^3 e^6}} \\ &= 35 - \frac{1}{2}\ln\left(\frac{n_{\mathrm{e}}}{10^{-2}\mathrm{cm}^{-3}}\right) + \frac{3}{2}\ln\left(\frac{k_{\mathrm{B}}T}{\mathrm{keV}}\right).\end{aligned}$$

- The value of t that implies $\langle\theta^2\rangle \approx 1$ is the deflection time t_{D},

$$\nu_{\mathrm{D}}^{\mathrm{ei}} = \frac{1}{t_{\mathrm{D}}^{\mathrm{ei}}} = n_{\mathrm{i}} 2\pi b_0^2 v_{\mathrm{e}} \ln\Lambda = \frac{8\pi n_{\mathrm{i}} Z^2 e^4}{m_{\mathrm{e}}^2 v_{\mathrm{e}}^3}\ln\Lambda \tag{3}$$

  and $\ln\Lambda \approx 35 \ldots 40$ in the ICM.
- This deflection frequency of small-angle scatterings is larger by a factor of $2\ln\Lambda \approx 70$ than the frequency of Eqn. (2), which is valid for a single large-angle scattering event $\Rightarrow$ small-scale, large-angle scatterings can be neglected!

Heat conduction – 4

- Back to our heat conductivity of electrons,

$$\kappa = \frac{n_\mathrm{e} v_\mathrm{e} c_V \lambda_\mathrm{mfp}}{3} = \frac{n_\mathrm{e} v_\mathrm{e} c_V}{3 \sigma n_\mathrm{i}}.$$

Heat conduction – 4

- Back to our heat conductivity of electrons,

$$\kappa = \frac{n_\mathrm{e} v_\mathrm{e} c_V \lambda_\mathrm{mfp}}{3} = \frac{n_\mathrm{e} v_\mathrm{e} c_V}{3\sigma n_\mathrm{i}}.$$

- From the equation of the deflection time due to many small-angle scattering events,

$$\nu_\mathrm{D}^\mathrm{ei} = \frac{1}{t_\mathrm{D}^\mathrm{ei}} = n_\mathrm{i} 2\pi b_0^2 v_\mathrm{e} \ln\Lambda = \frac{8\pi n_\mathrm{i} Z^2 e^4}{m_\mathrm{e}^2 v_\mathrm{e}^3} \ln\Lambda,$$

we can read off σ by remembering $\nu_\mathrm{D} = n_\mathrm{i}\sigma v_\mathrm{e}$:

$$\sigma = 2\pi b_0^2 \ln\Lambda = \frac{8\pi Z^2 e^4 \ln\Lambda}{m_\mathrm{e}^2 v_\mathrm{e}^4}.$$

Heat conduction – 4

- Back to our heat conductivity of electrons,

$$\kappa = \frac{n_\mathrm{e} v_\mathrm{e} c_V \lambda_\mathrm{mfp}}{3} = \frac{n_\mathrm{e} v_\mathrm{e} c_V}{3\sigma n_\mathrm{i}}.$$

- From the equation of the deflection time due to many small-angle scattering events,

$$\nu_\mathrm{D}^\mathrm{ei} = \frac{1}{t_\mathrm{D}^\mathrm{ei}} = n_\mathrm{i} 2\pi b_0^2 v_\mathrm{e} \ln\Lambda = \frac{8\pi n_\mathrm{i} Z^2 e^4}{m_\mathrm{e}^2 v_\mathrm{e}^3} \ln\Lambda,$$

  we can read off σ by remembering $\nu_\mathrm{D} = n_\mathrm{i}\sigma v_\mathrm{e}$:

$$\sigma = 2\pi b_0^2 \ln\Lambda = \frac{8\pi Z^2 e^4 \ln\Lambda}{m_\mathrm{e}^2 v_\mathrm{e}^4}.$$

- This yields the heat conductivity of electrons that are scattered by ions in a thermal gas,

$$\kappa = \frac{n_\mathrm{e} v_\mathrm{e}}{3} c_V \frac{m_\mathrm{e}^2 v_\mathrm{e}^4}{8\pi n_\mathrm{i} Z^2 e^4 \ln\Lambda} = \frac{1}{3}\left(\frac{m_\mathrm{e}^2}{8\pi Z^2 e^4}\right)\left(\frac{n_\mathrm{e}}{n_\mathrm{i}}\right)\frac{c_V v_\mathrm{e}^5}{\ln\Lambda}.$$

Heat conduction – 5

- Recap the expression for the heat conductivity of electrons,

$$\kappa = \frac{n_\mathrm{e} v_\mathrm{e}}{3} c_V \frac{m_\mathrm{e}^2 v_\mathrm{e}^4}{8\pi n_\mathrm{i} Z^2 e^4 \ln \Lambda} = \frac{1}{3} \left(\frac{m_\mathrm{e}^2}{8\pi Z^2 e^4} \right) \left(\frac{n_\mathrm{e}}{n_\mathrm{i}} \right) \frac{c_V v_\mathrm{e}^5}{\ln \Lambda}. \tag{4}$$

Heat conduction – 5

- Recap the expression for the heat conductivity of electrons,

$$\kappa = \frac{n_\mathrm{e} v_\mathrm{e}}{3} c_V \frac{m_\mathrm{e}^2 v_\mathrm{e}^4}{8\pi n_\mathrm{i} Z^2 e^4 \ln\Lambda} = \frac{1}{3}\left(\frac{m_\mathrm{e}^2}{8\pi Z^2 e^4}\right)\left(\frac{n_\mathrm{e}}{n_\mathrm{i}}\right)\frac{c_V v_\mathrm{e}^5}{\ln\Lambda}. \tag{4}$$

- The heat capacity at constant volume is $c_V = 3k_\mathrm{B}/2$ and the thermal electron velocity is $v_\mathrm{e} = \sqrt{2k_\mathrm{B}T_\mathrm{e}/m_\mathrm{e}}$. Inserting these expressions into Eqn. (4) yields a value for the heat conductivity

$$\begin{aligned}\kappa &= \frac{k_\mathrm{B}}{2}\left(\frac{m_\mathrm{e}^2}{8\pi Z^2 e^4}\right)\left(\frac{n_\mathrm{e}}{n_\mathrm{i}}\right)\left(\frac{2k_\mathrm{B}T_\mathrm{e}}{m_\mathrm{e}}\right)^{5/2}\frac{1}{\ln\Lambda} \\ &= 6.2\times10^{12}\left(\frac{T}{10^8\,\mathrm{K}}\right)^{5/2}\left(\frac{\ln\Lambda}{35}\right)^{-1}\frac{\mathrm{erg}}{\mathrm{s\,K\,cm}},\end{aligned}$$

where we used values for the Coulomb logarithm in cool core regions in clusters.

Heat conduction – 5

- Recap the expression for the heat conductivity of electrons,

$$\kappa = \frac{n_\mathrm{e} v_\mathrm{e}}{3} c_V \frac{m_\mathrm{e}^2 v_\mathrm{e}^4}{8\pi n_\mathrm{i} Z^2 e^4 \ln\Lambda} = \frac{1}{3}\left(\frac{m_\mathrm{e}^2}{8\pi Z^2 e^4}\right)\left(\frac{n_\mathrm{e}}{n_\mathrm{i}}\right)\frac{c_V v_\mathrm{e}^5}{\ln\Lambda}. \tag{4}$$

- The heat capacity at constant volume is $c_V = 3k_\mathrm{B}/2$ and the thermal electron velocity is $v_\mathrm{e} = \sqrt{2k_\mathrm{B}T_\mathrm{e}/m_\mathrm{e}}$. Inserting these expressions into Eqn. (4) yields a value for the heat conductivity

$$\begin{aligned}\kappa &= \frac{k_\mathrm{B}}{2}\left(\frac{m_\mathrm{e}^2}{8\pi Z^2 e^4}\right)\left(\frac{n_\mathrm{e}}{n_\mathrm{i}}\right)\left(\frac{2k_\mathrm{B}T_\mathrm{e}}{m_\mathrm{e}}\right)^{5/2}\frac{1}{\ln\Lambda} \\ &= 6.2\times10^{12}\left(\frac{T}{10^8\,\mathrm{K}}\right)^{5/2}\left(\frac{\ln\Lambda}{35}\right)^{-1}\frac{\mathrm{erg}}{\mathrm{s\,K\,cm}},\end{aligned}$$

  where we used values for the Coulomb logarithm in cool core regions in clusters.
- The strong temperature dependence of κ is a consequence of the velocity dependence ($\kappa \propto T^{5/2} \propto v_\mathrm{e}^5$). Four powers of which derive from the cross section $\sigma \propto b_0^2$ where $b_0 \equiv 2Ze^2/(m_\mathrm{e}v_\mathrm{e}^2)$ results from balancing the kinetic energy with the potential energy during a scattering event and one power results from $\kappa \propto v_\mathrm{e}\lambda_\mathrm{mfp}/3$, so that the conductive heat flux scales as $\boldsymbol{Q} = \kappa\boldsymbol{\nabla}T \propto T^{7/2}$.

Heat conduction – 5

- Recap the expression for the heat conductivity of electrons,

$$\kappa = \frac{n_\mathrm{e} v_\mathrm{e}}{3} c_V \frac{m_\mathrm{e}^2 v_\mathrm{e}^4}{8\pi n_\mathrm{i} Z^2 e^4 \ln\Lambda} = \frac{1}{3}\left(\frac{m_\mathrm{e}^2}{8\pi Z^2 e^4}\right)\left(\frac{n_\mathrm{e}}{n_\mathrm{i}}\right)\frac{c_V v_\mathrm{e}^5}{\ln\Lambda}. \tag{4}$$

- The heat capacity at constant volume is $c_V = 3k_\mathrm{B}/2$ and the thermal electron velocity is $v_\mathrm{e} = \sqrt{2k_\mathrm{B}T_\mathrm{e}/m_\mathrm{e}}$. Inserting these expressions into Eqn. (4) yields a value for the heat conductivity

$$\begin{aligned}\kappa &= \frac{k_\mathrm{B}}{2}\left(\frac{m_\mathrm{e}^2}{8\pi Z^2 e^4}\right)\left(\frac{n_\mathrm{e}}{n_\mathrm{i}}\right)\left(\frac{2k_\mathrm{B}T_\mathrm{e}}{m_\mathrm{e}}\right)^{5/2}\frac{1}{\ln\Lambda} \\ &= 6.2\times10^{12}\left(\frac{T}{10^8\,\mathrm{K}}\right)^{5/2}\left(\frac{\ln\Lambda}{35}\right)^{-1}\frac{\mathrm{erg}}{\mathrm{s\,K\,cm}},\end{aligned}$$

  where we used values for the Coulomb logarithm in cool core regions in clusters.
- The strong temperature dependence of κ is a consequence of the velocity dependence ($\kappa \propto T^{5/2} \propto v_\mathrm{e}^5$). Four powers of which derive from the cross section $\sigma \propto b_0^2$ where $b_0 \equiv 2Ze^2/(m_\mathrm{e}v_\mathrm{e}^2)$ results from balancing the kinetic energy with the potential energy during a scattering event and one power results from $\kappa \propto v_\mathrm{e}\lambda_\mathrm{mfp}/3$, so that the conductive heat flux scales as $\boldsymbol{Q} = \kappa\boldsymbol{\nabla}T \propto T^{7/2}$.
- The critical physics assumption behind this derivation of conduction is the random walk of electrons (along a field line) $\Rightarrow$ plasma physics modifies this!

Thermal instability: Field length – 1

- Cool star forming clouds should only appear in systems whose size is *greater* than a critical length scale, known as the *Field length* below which thermal conduction smoothes out temperature inhomogeneities.

Thermal instability: Field length – 1

- Cool star forming clouds should only appear in systems whose size is *greater* than a critical length scale, known as the *Field length* below which thermal conduction smoothes out temperature inhomogeneities.
- Formally we would have to a Lagrangian perturbation analysis to derive this length scale. Instead, we will derive the Field length heuristically by considering thermal balance for a cool cloud of radius r embedded in a medium of temperature T.

Thermal instability: Field length – 1

- Cool star forming clouds should only appear in systems whose size is *greater* than a critical length scale, known as the *Field length* below which thermal conduction smoothes out temperature inhomogeneities.
- Formally we would have to a Lagrangian perturbation analysis to derive this length scale. Instead, we will derive the Field length heuristically by considering thermal balance for a cool cloud of radius r embedded in a medium of temperature T.
- Electron thermal conduction sends energy into the cloud at a rate

$$\mathcal{H}_{\rm cond} \sim r^2 \kappa(T) \frac{T}{r} \sim \kappa_0 f_{\rm e} r \frac{T^{7/2}}{T_8^{5/2}}$$

Here, $T_8 = 10^8$ K, $f_{\rm e}$ is a magnetic suppression factor that depends on the topology of magnetic field lines connecting our cloud of consideration, and we used the *Spitzer conductivity* (which assumes a value for the Coulomb logarithm of $\ln \Lambda = 35$),

$$\kappa = 6.2 \times 10^{12} \left(\frac{T}{10^8\,\mathrm{K}}\right)^{5/2} f_{\rm e} \frac{\mathrm{erg}}{\mathrm{s\,K\,cm}} = \kappa_0 f_{\rm e} \left(\frac{T}{T_8}\right)^{5/2}.$$

Thermal instability: Field length – 2

- Radiative cooling can radiate away energy at a rate

$$\mathcal{C}_{\rm rad} \sim r^3 n_{\rm H}^2 \Lambda_0(T) \sim r^3 n_{\rm H}^2 \Lambda_0 \left(\frac{T}{T_8}\right)^{1/2}, \text{ with}$$

$$\Lambda_0(T) \approx 2.5 \times 10^{-23} \left(\frac{T}{T_8}\right)^{1/2} \frac{\text{erg cm}^3}{\text{s}}.$$

Thermal instability: Field length – 2

- Radiative cooling can radiate away energy at a rate

$$\mathcal{C}_{\rm rad} \sim r^3 n_{\rm H}^2 \Lambda_0(T) \sim r^3 n_{\rm H}^2 \Lambda_0 \left(\frac{T}{T_8}\right)^{1/2}, \text{ with}$$

$$\Lambda_0(T) \approx 2.5 \times 10^{-23} \left(\frac{T}{T_8}\right)^{1/2} \frac{\text{erg cm}^3}{\text{s}}.$$

- Cooling and conduction are thus in approximate balance, $\mathcal{H}_{\rm cond} \sim \mathcal{C}_{\rm rad}$, for systems with a radius of order the Field length

$$\lambda_{\rm F} \equiv \left[\frac{T\kappa(T)}{n_{\rm H}^2 \Lambda_0(T)}\right]^{1/2} = \left(\frac{\kappa_0 f_{\rm e} x_{\rm e}^2}{k_{\rm B} \Lambda_0 k_{\rm B}^2 T_8^2}\right)^{1/2} K_{\rm e}^{3/2}$$

$$\approx 6.6\,\text{kpc} \left(\frac{K_{\rm e}}{20\,\text{keV cm}^2}\right)^{3/2} f_{\rm e}^{1/2},$$

where we have used $K_{\rm e} = k_{\rm B} T / n_{\rm e}^{2/3}$ and the square of the hydrogen number density is given by $n_{\rm H}^2 = X_{\rm H}^2 \rho^2 / m_{\rm p}^2 = n_{\rm e}^2 / x_{\rm e}^2$.

Thermal instability: Field length – 2

- Radiative cooling can radiate away energy at a rate

$$\mathcal{C}_{\rm rad} \sim r^3 n_{\rm H}^2 \Lambda_0(T) \sim r^3 n_{\rm H}^2 \Lambda_0 \left(\frac{T}{T_8}\right)^{1/2}, \text{ with}$$

$$\Lambda_0(T) \approx 2.5 \times 10^{-23} \left(\frac{T}{T_8}\right)^{1/2} \frac{\text{erg cm}^3}{\text{s}}.$$

- Cooling and conduction are thus in approximate balance, $\mathcal{H}_{\rm cond} \sim \mathcal{C}_{\rm rad}$, for systems with a radius of order the Field length

$$\lambda_{\rm F} \equiv \left[\frac{T\kappa(T)}{n_{\rm H}^2 \Lambda_0(T)}\right]^{1/2} = \left(\frac{\kappa_0 f_{\rm e} x_{\rm e}^2}{k_{\rm B} \Lambda_0 k_{\rm B}^2 T_8^2}\right)^{1/2} K_{\rm e}^{3/2}$$

$$\approx 6.6\,\text{kpc} \left(\frac{K_{\rm e}}{20\,\text{keV cm}^2}\right)^{3/2} f_{\rm e}^{1/2},$$

where we have used $K_{\rm e} = k_{\rm B} T / n_{\rm e}^{2/3}$ and the square of the hydrogen number density is given by $n_{\rm H}^2 = X_{\rm H}^2 \rho^2 / m_{\rm p}^2 = n_{\rm e}^2 / x_{\rm e}^2$.

- ***Through a coincidence of scaling, the Field length is a function of entropy alone when free-free emission is the dominant cooling mechanism.***

Thermal instability: Field length – 3

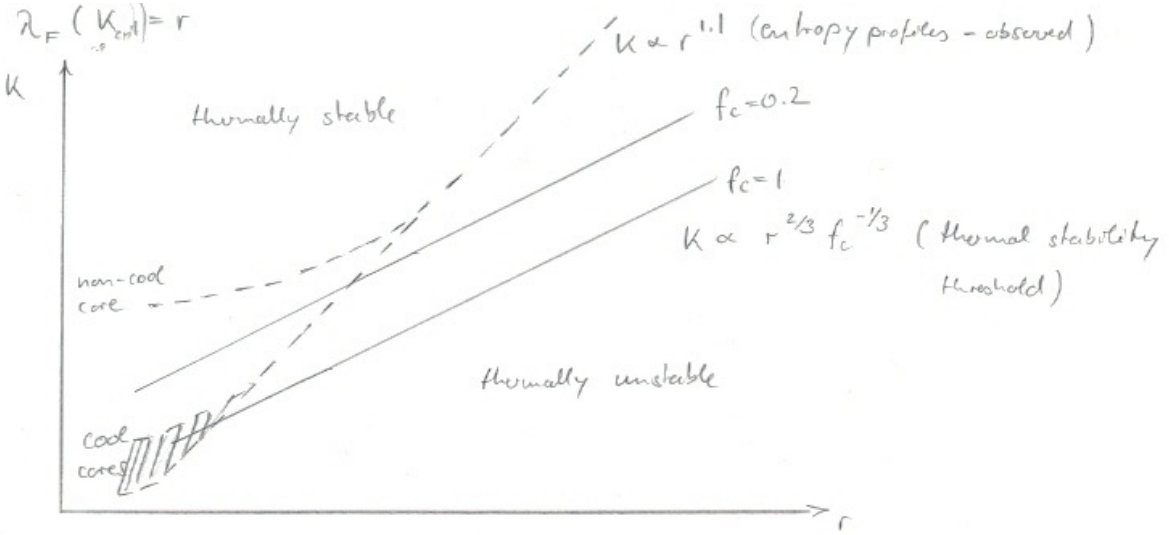

- We can translate this criterion in the entropy-radius plane by adopting $\lambda_F(K) = r$. This yields a thermal stability threshold that obeys a scaling with radius of $K \propto r^{2/3} f_e^{-1/3} = \lambda_F^{2/3} f_e^{-1/3}$.

Thermal instability: Field length – 3

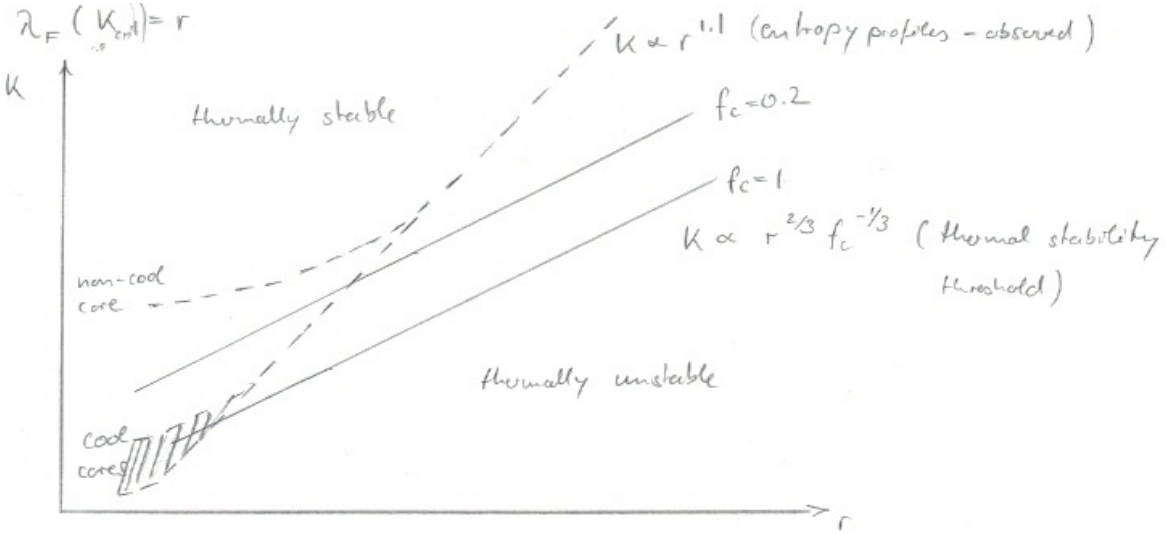

- We can translate this criterion in the entropy-radius plane by adopting $\lambda_F(K) = r$. This yields a thermal stability threshold that obeys a scaling with radius of $K \propto r^{2/3} f_e^{-1/3} = \lambda_F^{2/3} f_e^{-1/3}$.
- Gas that is below that threshold and resides within radius r constitutes a subsystem with $r > \lambda_F$ (at constant K), i.e., the amount of entropy in the larger cloud is too small to support fast enough conduction that is necessary to prevent a cooling run-away, allowing multiphase gas to persist and star formation to proceed.

Thermal instability: Field length – 3

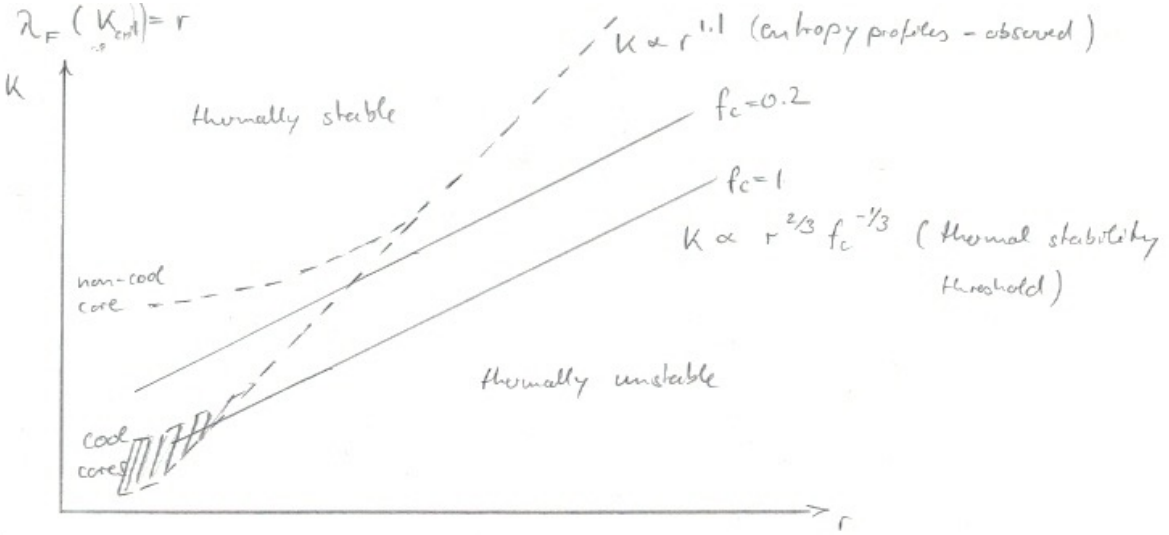

- We can translate this criterion in the entropy-radius plane by adopting $\lambda_F(K) = r$. This yields a thermal stability threshold that obeys a scaling with radius of $K \propto r^{2/3} f_e^{-1/3} = \lambda_F^{2/3} f_e^{-1/3}$.
- Gas that is below that threshold and resides within radius r constitutes a subsystem with $r > \lambda_F$ (at constant K), i.e., the amount of entropy in the larger cloud is too small to support fast enough conduction that is necessary to prevent a cooling run-away, allowing multiphase gas to persist and star formation to proceed.
- Gas above the threshold resides in the region of thermal stability in which conduction is fast enough and leads to evaporation of a cool cloud and eventually homogeneity.

Thermal instability: Field length – 4

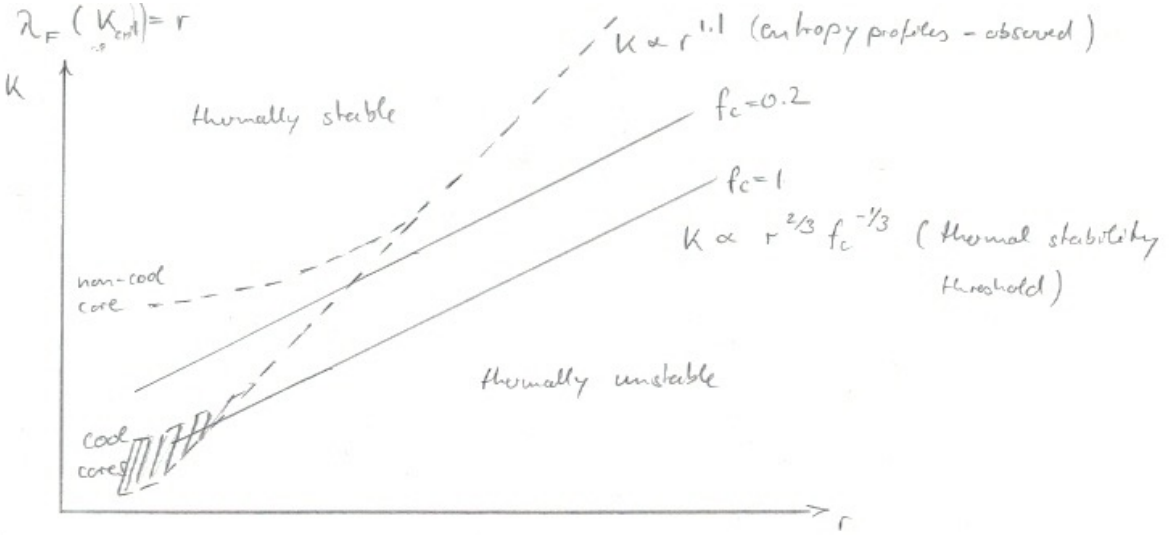

- While studying *entropy generation by accretion*, we found that the entropy profile of the ICM at larger scales shows the behavior $K \propto r^{1.1}$. This leaves us with two possibilities of cluster states in reality (which appear to be dynamical attractor solutions of thermal stability considerations).

Thermal instability: Field length – 4

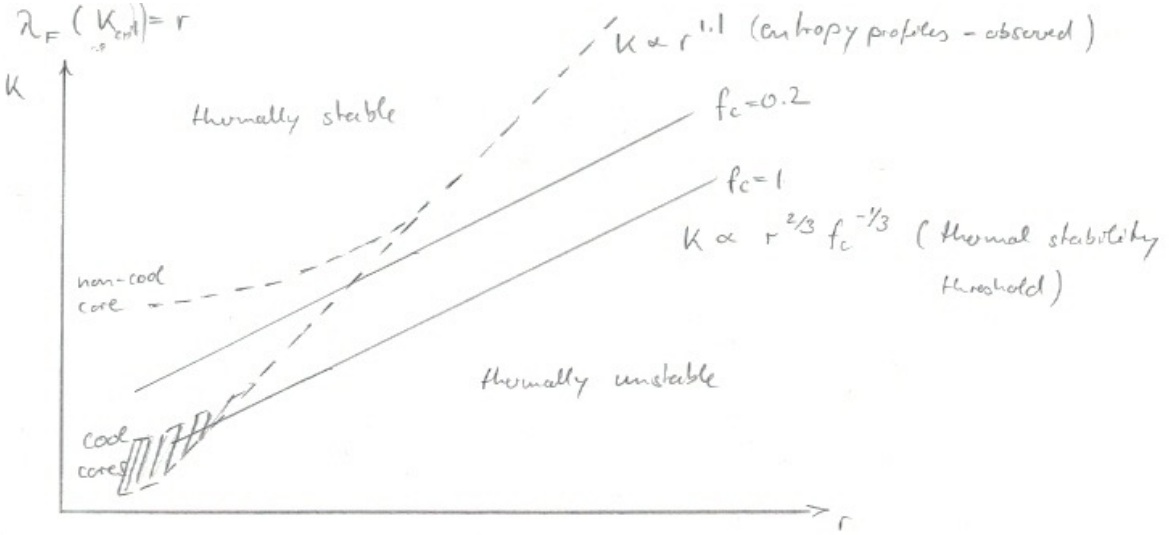

- While studying *entropy generation by accretion*, we found that the entropy profile of the ICM at larger scales shows the behavior $K \propto r^{1.1}$. This leaves us with two possibilities of cluster states in reality (which appear to be dynamical attractor solutions of thermal stability considerations).
- Clusters can have an entropy profile that always stays above the thermal stability threshold. As a consequence, the steeper entropy profile on larger scale necessarily needs to break at sufficiently large radii to join an elevated level of central entropy. This defines the class of ***non-cool core clusters***.

Thermal instability: Field length – 4

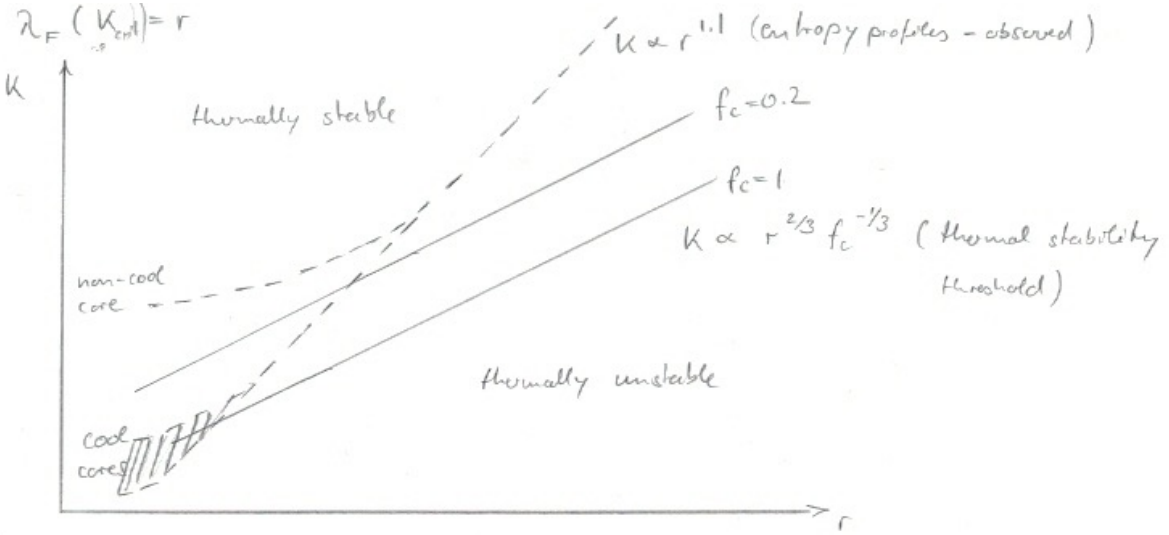

- While studying *entropy generation by accretion*, we found that the entropy profile of the ICM at larger scales shows the behavior $K \propto r^{1.1}$. This leaves us with two possibilities of cluster states in reality (which appear to be dynamical attractor solutions of thermal stability considerations).
- Clusters can have an entropy profile that always stays above the thermal stability threshold. As a consequence, the steeper entropy profile on larger scale necessarily needs to break at sufficiently large radii to join an elevated level of central entropy. This defines the class of ***non-cool core clusters***.
- Clusters can have an entropy profile that continues to decrease toward smaller radii until it drops below the thermal stability threshold. There the gas is subject to thermal instability, and multiphase gas can form, potentially seeding star formation. This constitutes the class of ***cool core clusters***.

Heating versus cooling: a visual stability analysis – 1

- Formally one needs to do a perturbation analysis of the hydrodynamic equations; here we will only sketch the concept and show the main ideas by introducing a visual stability analysis.

Heating versus cooling: a visual stability analysis – 1

- Formally one needs to do a perturbation analysis of the hydrodynamic equations; here we will only sketch the concept and show the main ideas by introducing a visual stability analysis.
- Because we allow for thermal conduction, the entropy of a fluid element is not any more conserved. Instead, we consider hydrostatic rearrangements that conserve the thermal pressure $P = nk_{\mathrm{B}}T$ and rewrite the energy deposition and cooling rates as functions of temperature and pressure.

Heating versus cooling: a visual stability analysis – 1

- Formally one needs to do a perturbation analysis of the hydrodynamic equations; here we will only sketch the concept and show the main ideas by introducing a visual stability analysis.
- Because we allow for thermal conduction, the entropy of a fluid element is not any more conserved. Instead, we consider hydrostatic rearrangements that conserve the thermal pressure $P = nk_{\rm B}T$ and rewrite the energy deposition and cooling rates as functions of temperature and pressure.
- We consider radiative cooling (bremsstrahlung and free-free line emission, denoted by $\mathcal{C}_{\rm rad}$) and heating by conduction ($\mathcal{H}_{\rm cond}$), turbulent dissipation ($\mathcal{H}_{\rm turb}$), and Coulomb and hadronic interactions of cosmic rays with the thermal gas ($\mathcal{H}_{\rm hadr}$) and find the scaling of the volumetric cooling and heating rates with T:

$$\mathcal{C}_{\rm rad} \propto r^3 n^2 \left[T^{1/2} + \Lambda_{\rm line}(T)\right] \propto P\left[T^{-1/2} + \frac{\Lambda_{\rm line}(T)}{T}\right],$$

$$\mathcal{H}_{\rm cond} \propto r^2 \kappa(T) \frac{T}{r} \propto r\, T^{7/2} \propto P^{-1/3} T^{23/6},$$

$$\mathcal{H}_{\rm turb} \propto r^3 n \propto T^0,$$

$$\mathcal{H}_{\rm hadr} \propto r^3 n n_{\rm cr} \propto f_{\rm cr} \frac{P}{T},$$

where $\Lambda_{\rm line}(T) \propto T^{\alpha_{\rm line}}$, $\alpha_{\rm line} < 1/2$ for $k_{\rm B}T < 2\,{\rm keV}$, and $f_{\rm cr} = n_{\rm cr}/n = {\rm const.}$

Heating versus cooling: a visual stability analysis – 2

- However, Coulomb and hadronic interactions of cosmic rays with the thermal gas are too slow $\Rightarrow \mathcal{H}_{\rm hadr} \ll \mathcal{C}_{\rm rad}$ and we cannot find a thermal equilibrium.
- More promising: cosmic ray streaming heating via the gyro-resonant excitation of Alfvén waves and damping heats the surrounding plasma at a rate:

$$\mathcal{H}_{\rm cr} \sim r^3 |\boldsymbol{v}_{\rm A} \cdot \boldsymbol{\nabla} P_{\rm cr}|$$

  where $\boldsymbol{v}_{\rm A} = \boldsymbol{B}/\sqrt{4\pi\rho}$ is the Alfvén velocity, $\boldsymbol{B}$ is the magnetic field, ρ is the mass density, and $P_{\rm cr}$ is the cosmic ray pressure.
- Assuming magnetic flux freezing for isotropic volume changes so that $B = \sqrt{\boldsymbol{B}^2} \propto n^{2/3}$, adiabatic cosmic rays so that $P_{\rm cr} \propto n^{4/3}$, and $r^2 \propto n^{-2/3}$, we obtain:

$$\mathcal{H}_{\rm cr} \propto r^3 \frac{B}{n^{1/2}} \frac{P_{\rm cr}}{r} \propto n^{-2/3+2/3-1/2+4/3} \propto n^{5/6} \propto \left(\frac{P}{T}\right)^{5/6}$$

Heating versus cooling: a visual stability analysis – 3

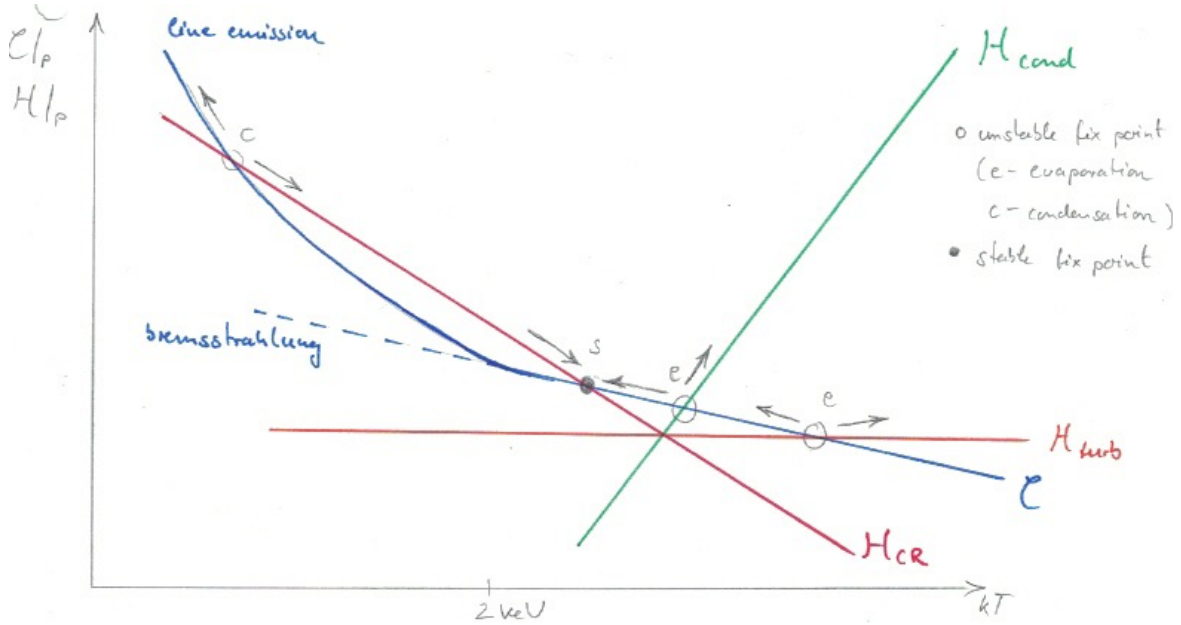

- We find the stability properties of the different heating processes by considering the energy deposition and cooling rates as a function of temperature.

Heating versus cooling: a visual stability analysis – 3

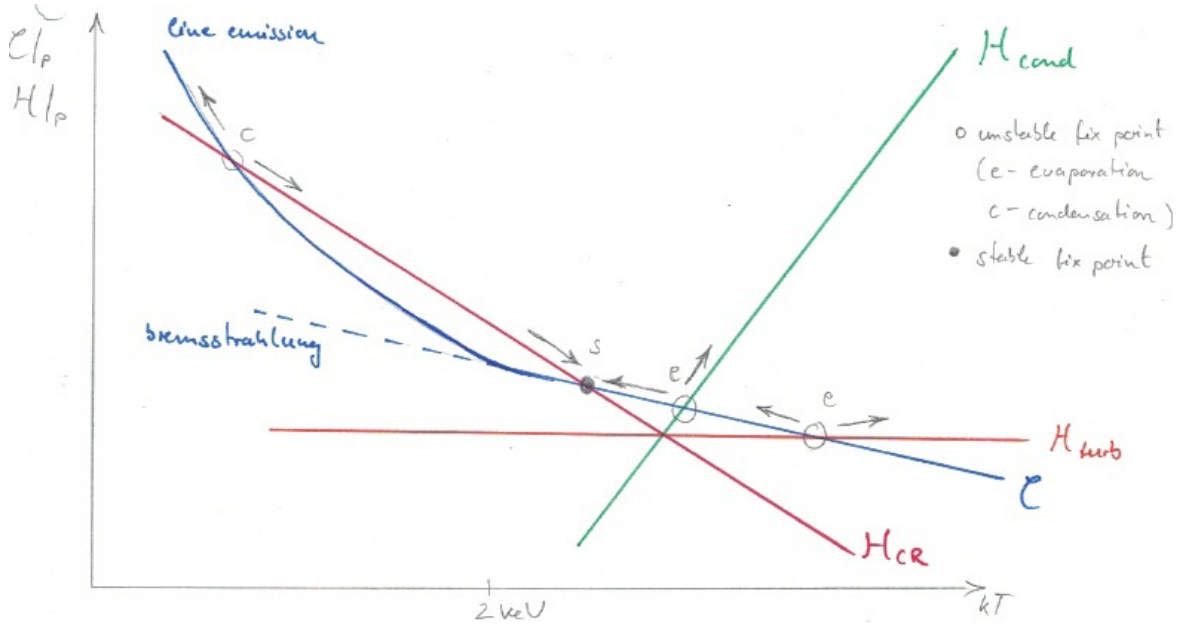

- We find the stability properties of the different heating processes by considering the energy deposition and cooling rates as a function of temperature.
- This clearly demonstrates that conductive and turbulent heating cannot be in stable equilibrium with radiative cooling. By contrast, a heating mechanism with an energy deposition rate that scales with $T^{-5/6}$ (such as cosmic ray streaming heating) allows for stable solutions.

Heating versus cooling: a visual stability analysis – 4

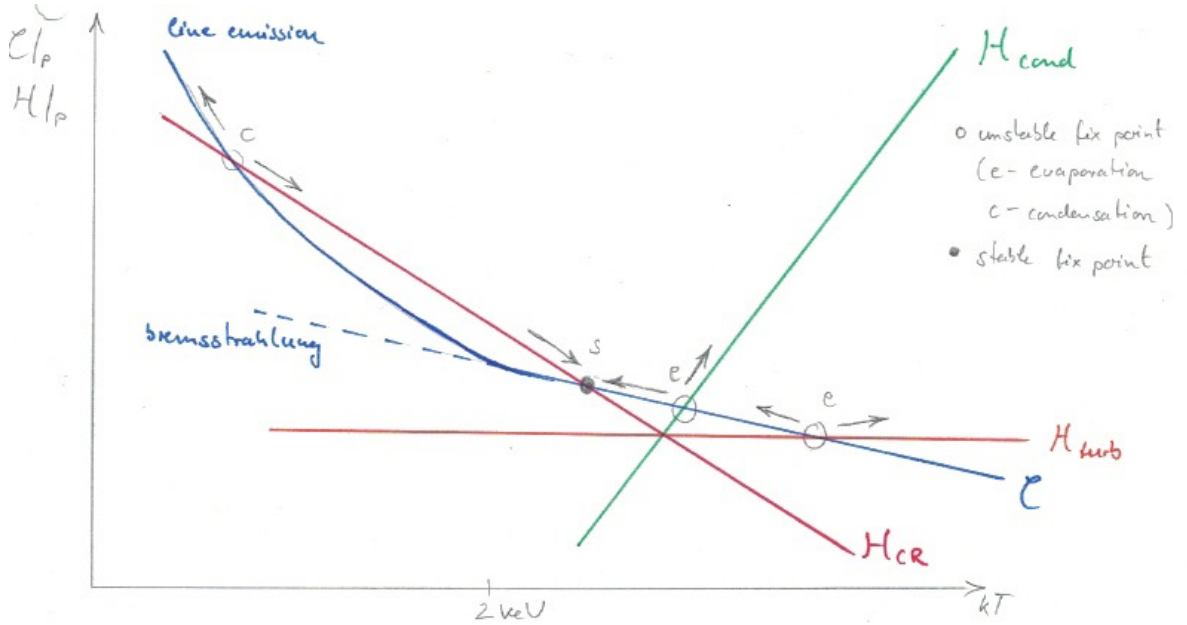

- Of course, the final state of the system depends on boundary conditions and conservation laws as discussed in the following.

Heating versus cooling: a visual stability analysis – 4

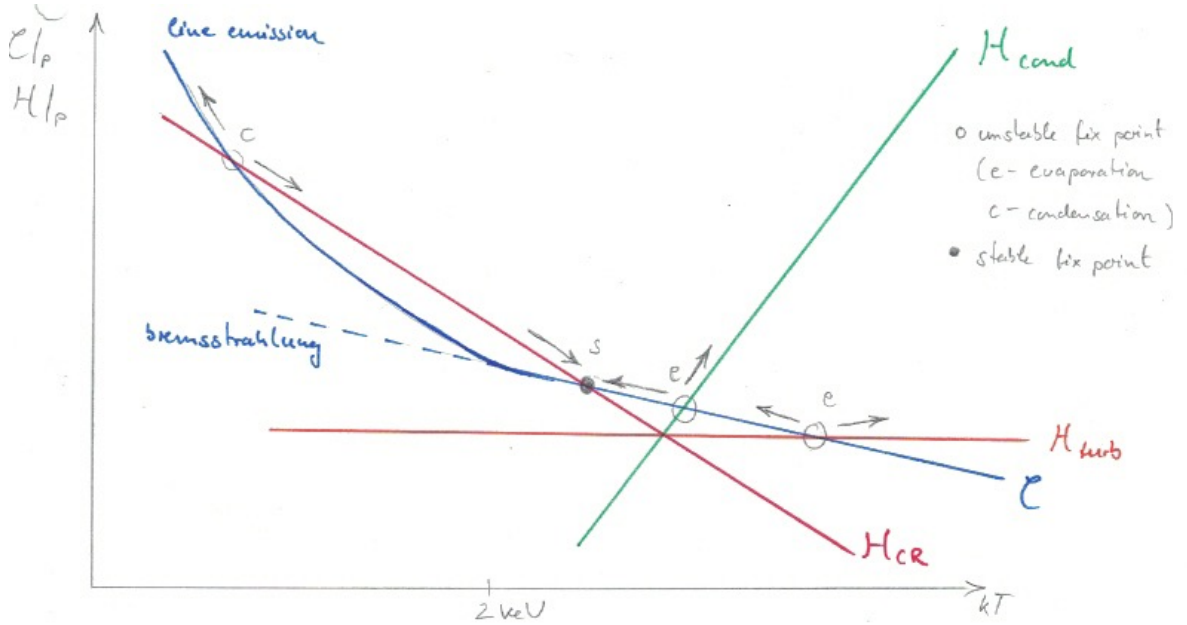

- Of course, the final state of the system depends on boundary conditions and conservation laws as discussed in the following.
- **Thermal conduction.** Here the free energy is borrowed from the temperature gradient ∇T and heating comes to an end once a constant temperature profile has been reached.
- **Turbulent dissipation** causes the temperature to increase until $3k_{\mathrm{B}}T \sim mv^2$ or if all turbulent kinetic energy has been dissipated.
- **Cosmic ray streaming** requires a source of cosmic rays close to the center and a sufficiently steep pressure gradient to provide a large enough cosmic ray flux.

Heating versus cooling: cosmic ray heating

- In order to estimate the ability of cosmic ray streaming heating to balance radiative cooling, we calculate the ratio of both rates:

$$\frac{\mathcal{H}_{\rm cr}}{\mathcal{C}_{\rm cool}} = \frac{|\boldsymbol{v}_{\rm A} \cdot \boldsymbol{\nabla} P_{\rm cr}|}{n^2 \Lambda(T)} \sim \frac{1}{\beta^{1/2}} \frac{P_{\rm cr}}{P_{\rm th}} \frac{H_{\rm th}}{H_{\rm cr}} \frac{\tau_{\rm cool}}{\tau_{\rm ff}} \sim \mathcal{O}(1),$$

  where $\beta = P_{\rm th}/P_B$ is the plasma β parameter, i.e., the ratio of thermal to magnetic pressure, $H_{\rm th}$ and $H_{\rm cr}$ are the scale heights of thermal and cosmic ray pressures, respectively, $\tau_{\rm cool}$ is the radiative cooling timescale of the ICM, and $\tau_{\rm ff} = H_{\rm gas}/c_{\rm sd}$ is the free-fall timescale (assuming approximate hydrostatic equilibrium and $c_{\rm sd}$ is the sound speed).
- Given that (i) typically $\beta \sim 10^2$, (ii) the cosmic ray pressure profile can be locally much steeper than the thermal gas profile, (we assume $H_{\rm th}/H_{\rm cr} \sim 10$ for the sake of the argument), (iii) $\tau_{\rm cool}/\tau_{\rm ff} \sim 10$ when the gas is locally thermally unstable as is often the case in cool cores, and (iv) the ratio of cosmic ray-to-gas pressure is small (here assumed to be 10% for the sake of the argument), this estimate shows that cosmic ray heating can be competitive with radiative cooling for reasonable choices of model parameters.

Thermal stability with magnetic fields

- In a ***weakly collisional magnetized plasma*** which we encounter in a galaxy cluster, electrons cannot move “freely” but are bound to follow and gyrate around magnetic field lines. This modifies the convective stability criterion and the type of instability depends on the sign of ∇T.

Thermal stability with magnetic fields

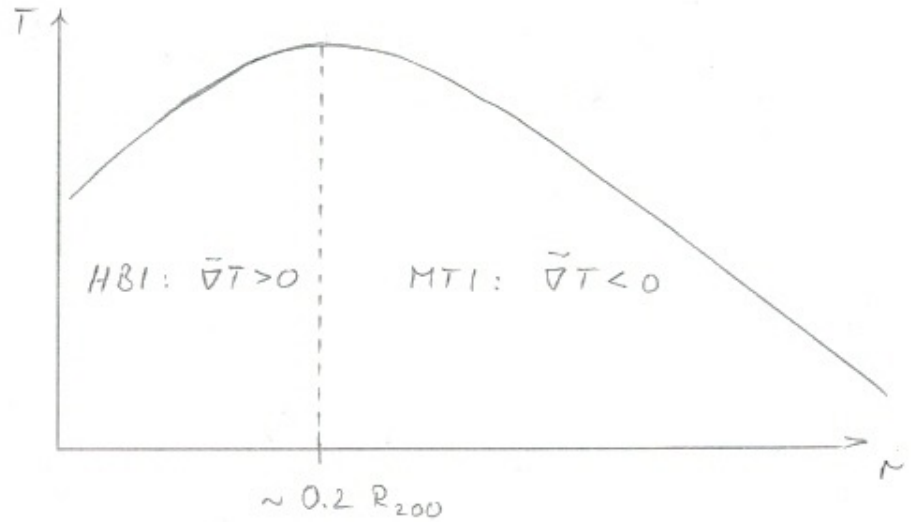

- In a ***weakly collisional magnetized plasma*** which we encounter in a galaxy cluster, electrons cannot move "freely" but are bound to follow and gyrate around magnetic field lines. This modifies the convective stability criterion and the type of instability depends on the sign of ∇T.
- In the center, $T(r)$ of a cool core cluster increases to reach a maximum at a radius of around $0.2\,R_{200}$ and decreases again towards larger radii.

AIP

Thermal stability with magnetic fields

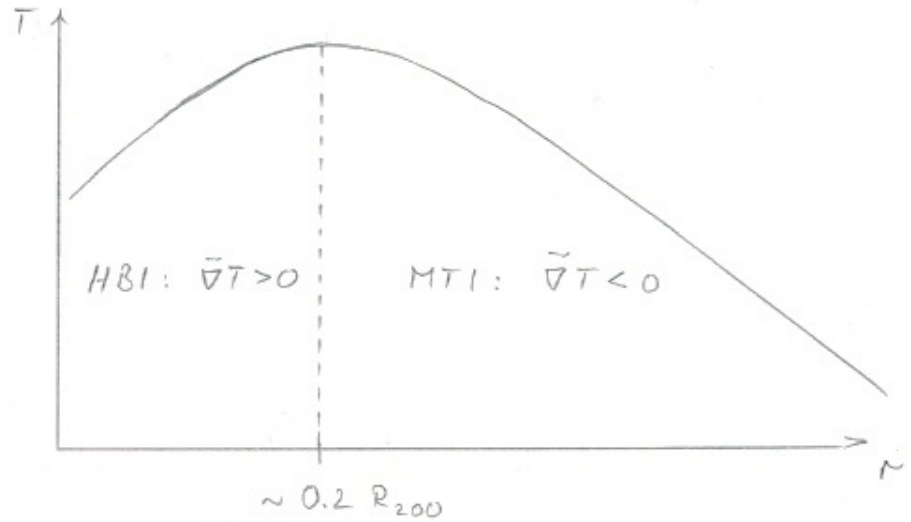

- In a ***weakly collisional magnetized plasma*** which we encounter in a galaxy cluster, electrons cannot move "freely" but are bound to follow and gyrate around magnetic field lines. This modifies the convective stability criterion and the type of instability depends on the sign of ∇T.
- In the center, $T(r)$ of a cool core cluster increases to reach a maximum at a radius of around $0.2\,R_{200}$ and decreases again towards larger radii.
- As will explain now, the magneto-thermal instability (MTI, Balbus 2001) can only be excited in the outer cluster regions where $\boldsymbol{e}_r \cdot \nabla T < 0$. Conversely, the heat-flux driven buoyancy instability (HBI, Quataert 2008) is excited in the cooling core region where $\boldsymbol{e}_r \cdot \nabla T > 0$.

Thermal stability with magnetic fields

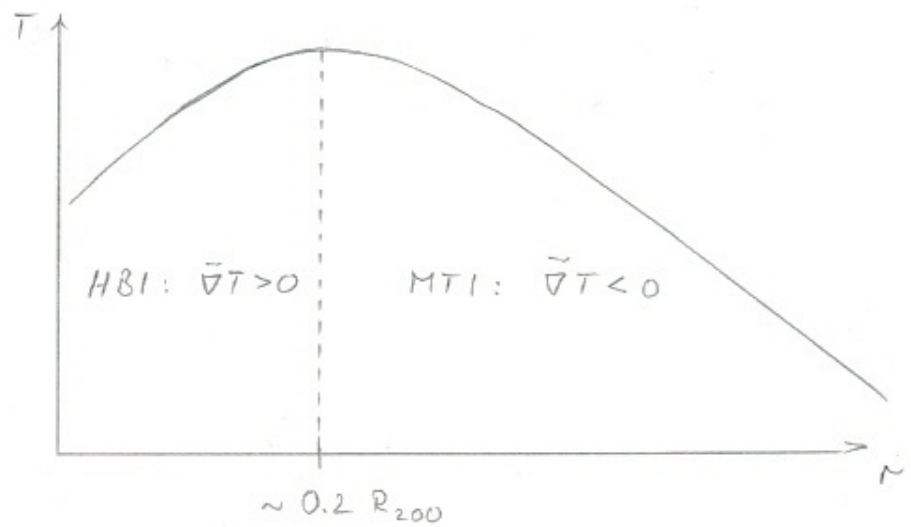

- In a ***weakly collisional magnetized plasma*** which we encounter in a galaxy cluster, electrons cannot move "freely" but are bound to follow and gyrate around magnetic field lines. This modifies the convective stability criterion and the type of instability depends on the sign of ∇T.
- In the center, $T(r)$ of a cool core cluster increases to reach a maximum at a radius of around $0.2\,R_{200}$ and decreases again towards larger radii.
- As will explain now, the magneto-thermal instability (MTI, Balbus 2001) can only be excited in the outer cluster regions where $\boldsymbol{e}_r \cdot \nabla T < 0$. Conversely, the heat-flux driven buoyancy instability (HBI, Quataert 2008) is excited in the cooling core region where $\boldsymbol{e}_r \cdot \nabla T > 0$.
- Note that both types of buoyancy instabilities would be absent without magnetic fields because the ICM is stably stratified according to the Schwarzschild criterion of convective stability because $\mathrm{d}S/\mathrm{d}r > 0$.

Magneto-thermal instability

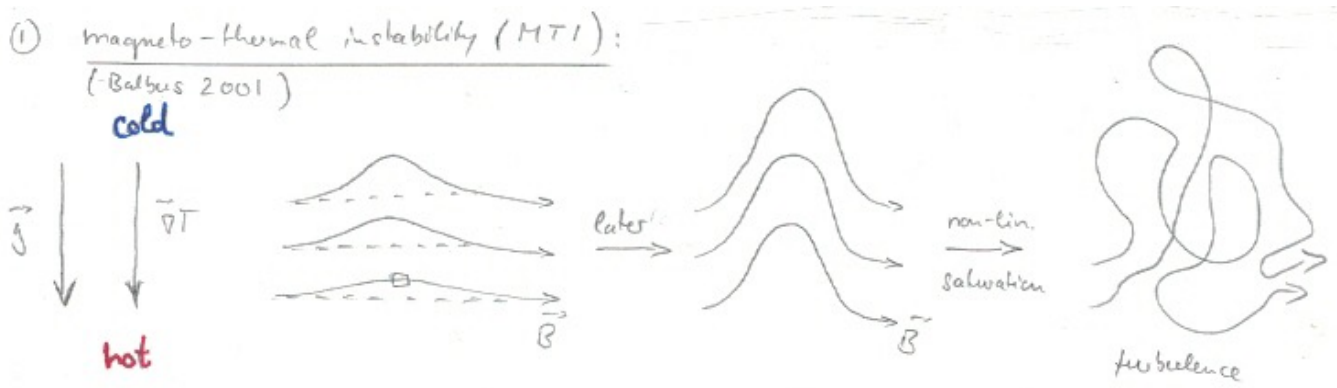

- We assume that magnetic fields are initially aligned horizontally (or only consider the horizontal magnetic field component). Displacing a volume element upwards in the gravitational potential would cause it to adiabatically expand and to cool in the absence of conduction.

Magneto-thermal instability

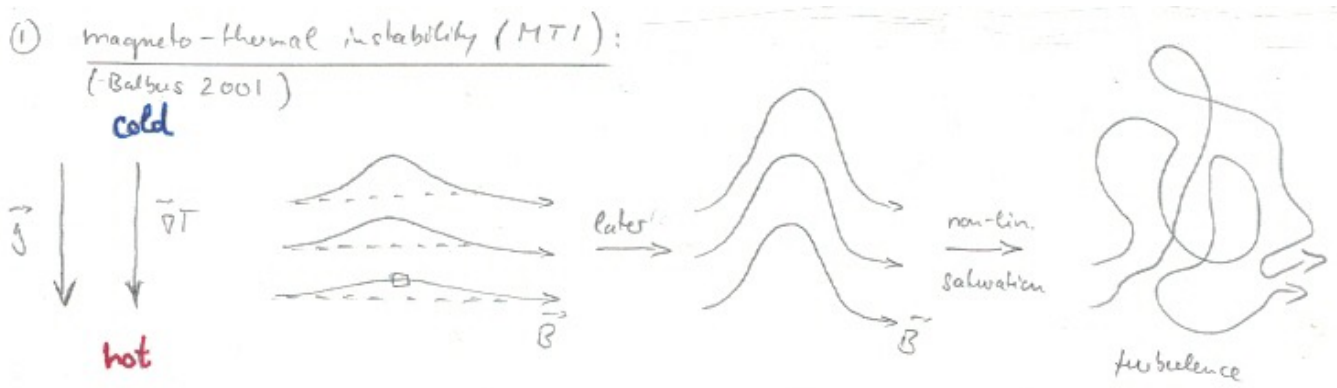

- We assume that magnetic fields are initially aligned horizontally (or only consider the horizontal magnetic field component). Displacing a volume element upwards in the gravitational potential would cause it to adiabatically expand and to cool in the absence of conduction.
- Instead, it is conductively heated from the hotter heat bath below to which it is connected by the magnetic field. This causes further expansion and dilution so that the volume element continues to rise as it remains lighter than the surrounding ICM. Hence, this dynamics reinforces the cause of the evolution, giving rise to instability.

Magneto-thermal instability

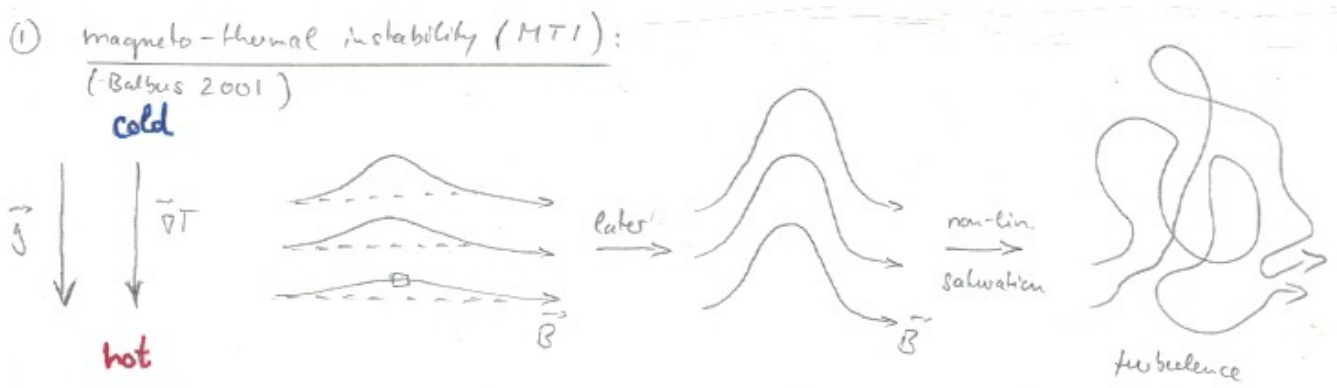

- We assume that magnetic fields are initially aligned horizontally (or only consider the horizontal magnetic field component). Displacing a volume element upwards in the gravitational potential would cause it to adiabatically expand and to cool in the absence of conduction.
- Instead, it is conductively heated from the hotter heat bath below to which it is connected by the magnetic field. This causes further expansion and dilution so that the volume element continues to rise as it remains lighter than the surrounding ICM. Hence, this dynamics reinforces the cause of the evolution, giving rise to instability.
- Non-linear simulations of the MTI show that it does not quiescently saturate with a radial field (as expected from the linear stability analysis) but in a turbulent state. The reason for this is that the radial field configuration is overstable, i.e., the magnetic field always overshoots this radial configuration while its amplitude continues to grow.

Heat-flux driven buoyancy instability – 1

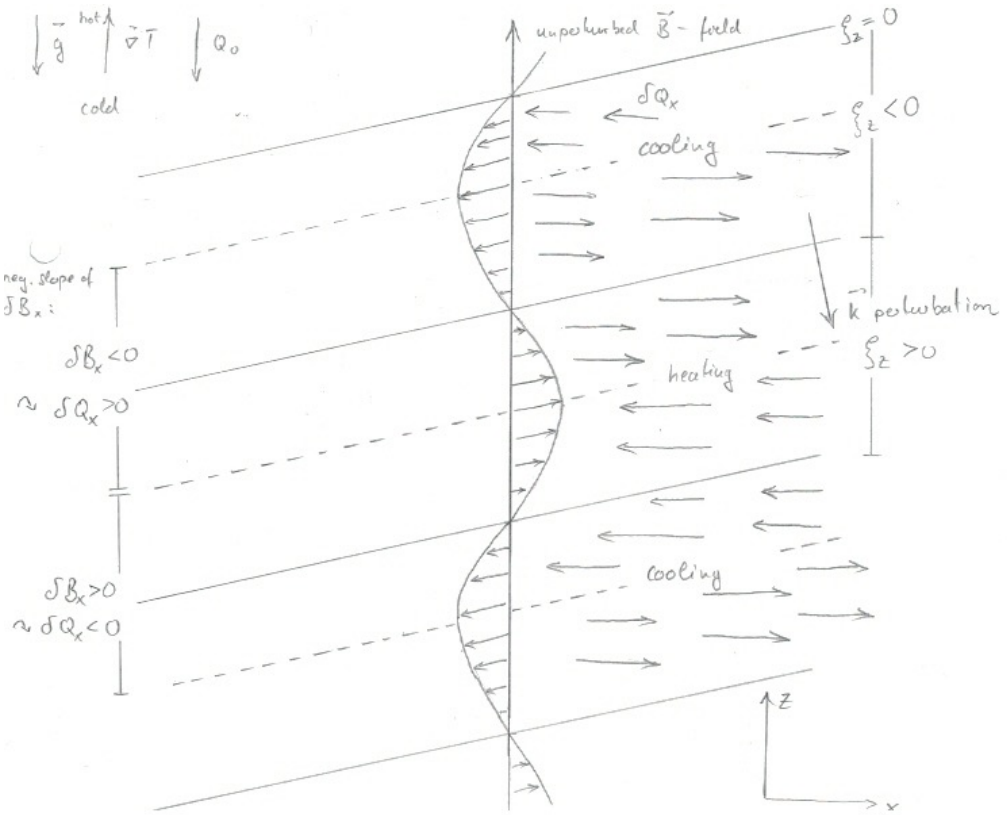

- If the temperature gradient is antiparallel to the direction of gravity, the ICM is susceptible to exciting the HBI. To understand this instability, we introduce the displacement field $\boldsymbol{\xi} \equiv \mathrm{i}\delta\boldsymbol{v}/\omega \propto \delta\boldsymbol{v}$.

AIP

Heat-flux driven buoyancy instability – 1

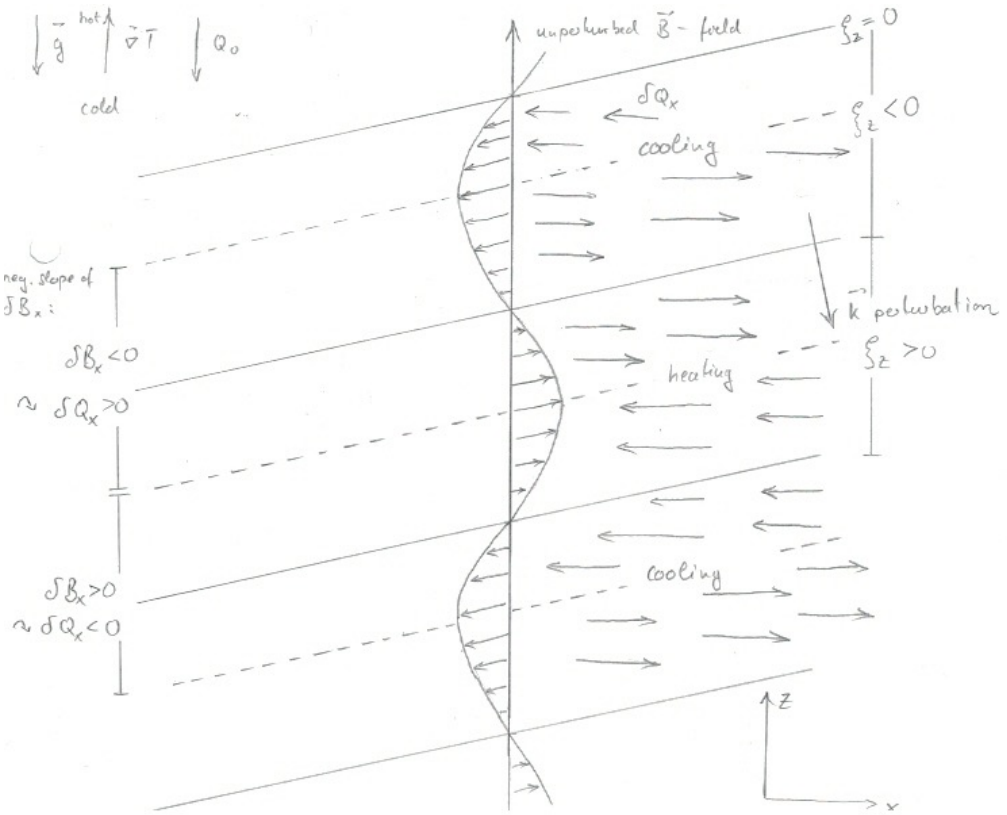

- If the temperature gradient is antiparallel to the direction of gravity, the ICM is susceptible to exciting the HBI. To understand this instability, we introduce the displacement field $\boldsymbol{\xi} \equiv \mathrm{i}\delta\boldsymbol{v}/\omega \propto \delta\boldsymbol{v}$.
- We assume incompressible gas, consider a Fourier transformed background at rest and perturbed quantities, so that $\boldsymbol{v}_0 = \boldsymbol{0}$ and find

$$\begin{aligned} & \boldsymbol{\nabla} \cdot \delta\boldsymbol{v} = 0 \\ \Rightarrow \quad & \boldsymbol{k} \cdot \delta\boldsymbol{v} = 0 \\ \Rightarrow \quad & \boldsymbol{k} \cdot \boldsymbol{\xi} = 0, \end{aligned}$$

i.e., $\boldsymbol{k}$ is perpendicular to $\boldsymbol{\xi}$.

Heat-flux driven buoyancy instability – 2

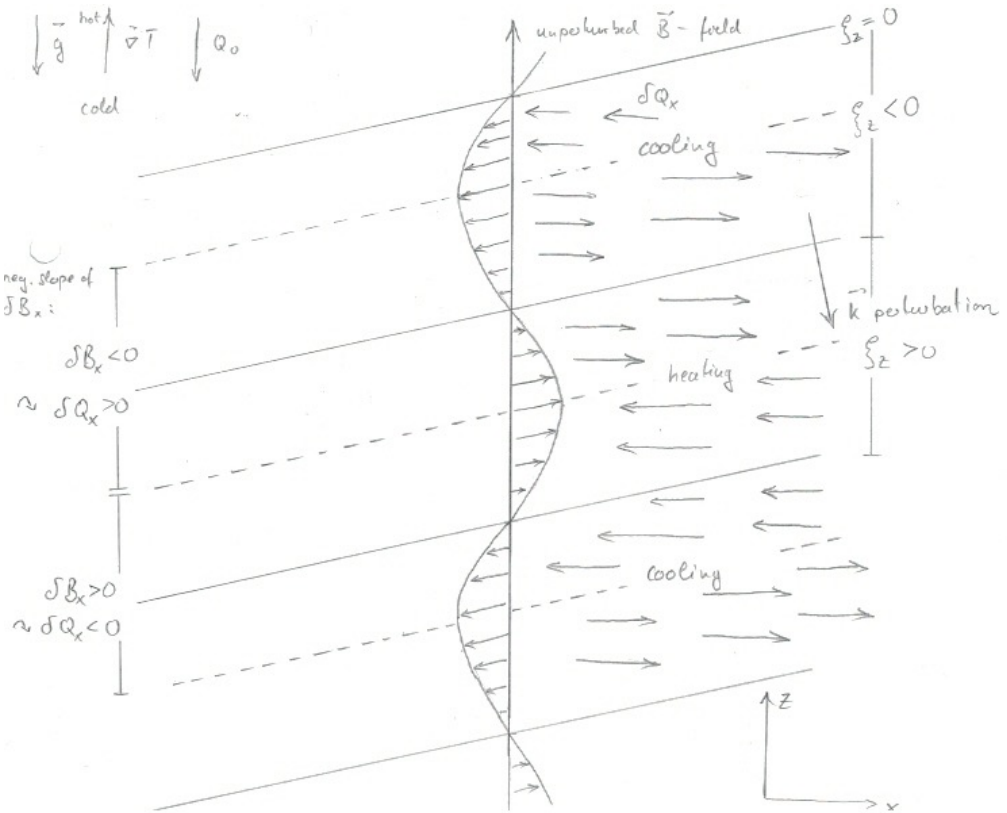

- If the temperature gradient increases outwards, there will be a background heat flux $\boldsymbol{Q}_0$ pointing inwards along the unperturbed radial magnetic field lines (our assumed initial state).

AIP

Heat-flux driven buoyancy instability – 2

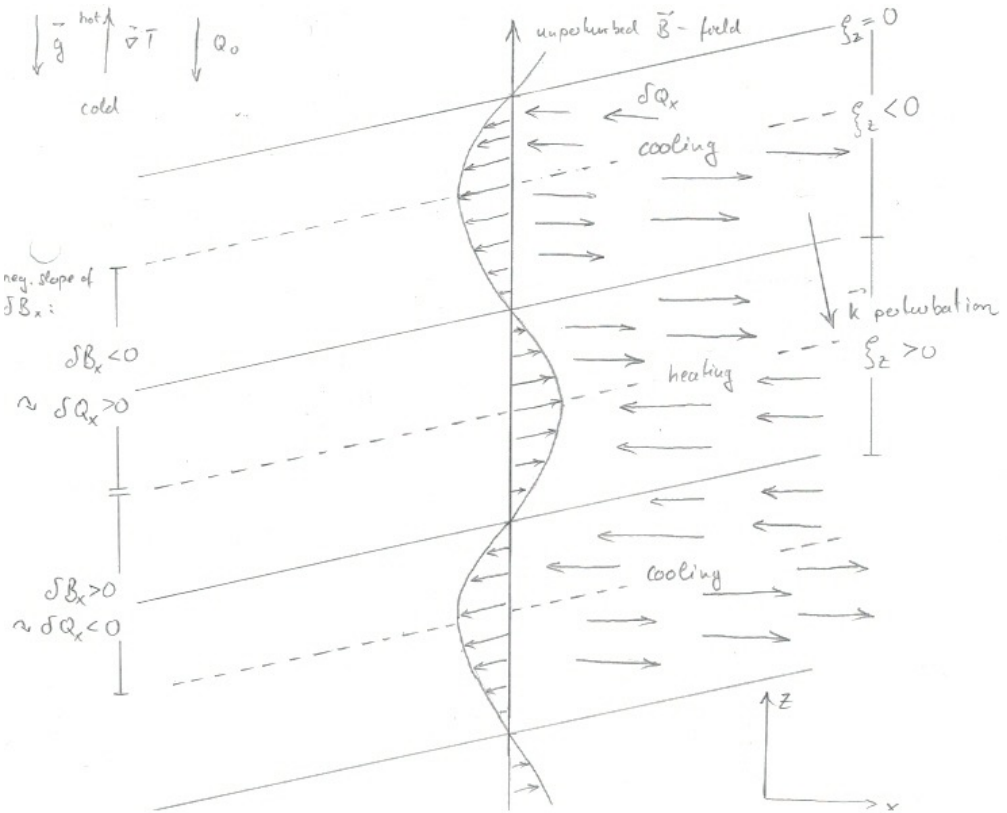

- If the temperature gradient increases outwards, there will be a background heat flux $\boldsymbol{Q}_0$ pointing inwards along the unperturbed radial magnetic field lines (our assumed initial state).
- Oblique perturbations with a wave vector $\boldsymbol{k}$ at some angle with the magnetic field yields $\delta\boldsymbol{B} \perp \boldsymbol{k}$ (because of $\nabla \cdot \delta\boldsymbol{v} = 0$).

AIP

Heat-flux driven buoyancy instability – 2

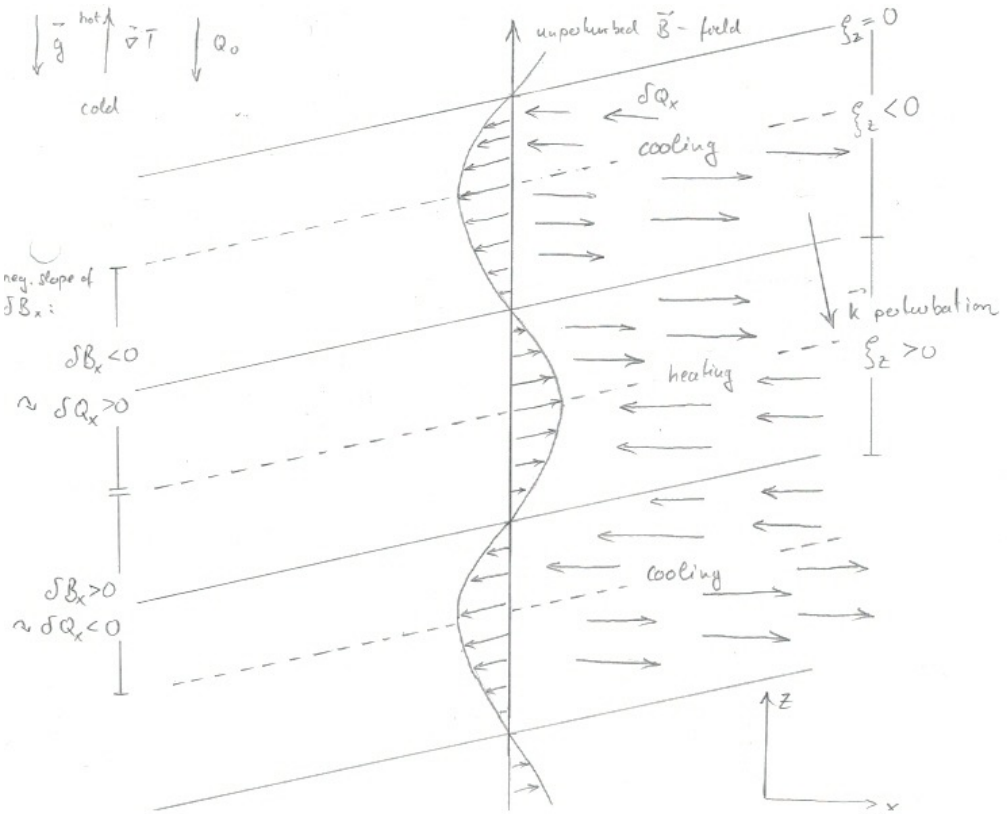

- If the temperature gradient increases outwards, there will be a background heat flux $\boldsymbol{Q}_0$ pointing inwards along the unperturbed radial magnetic field lines (our assumed initial state).
- Oblique perturbations with a wave vector $\boldsymbol{k}$ at some angle with the magnetic field yields $\delta\boldsymbol{B} \perp \boldsymbol{k}$ (because of $\nabla \cdot \delta\boldsymbol{v} = 0$).
- In the figure, we work out the perturbations to the heat flux along the x direction, δQ_x, in response to the displaced component of the magnetic field, B_x, that is flux-frozen into the cluster plasma.

Heat-flux driven buoyancy instability – 3

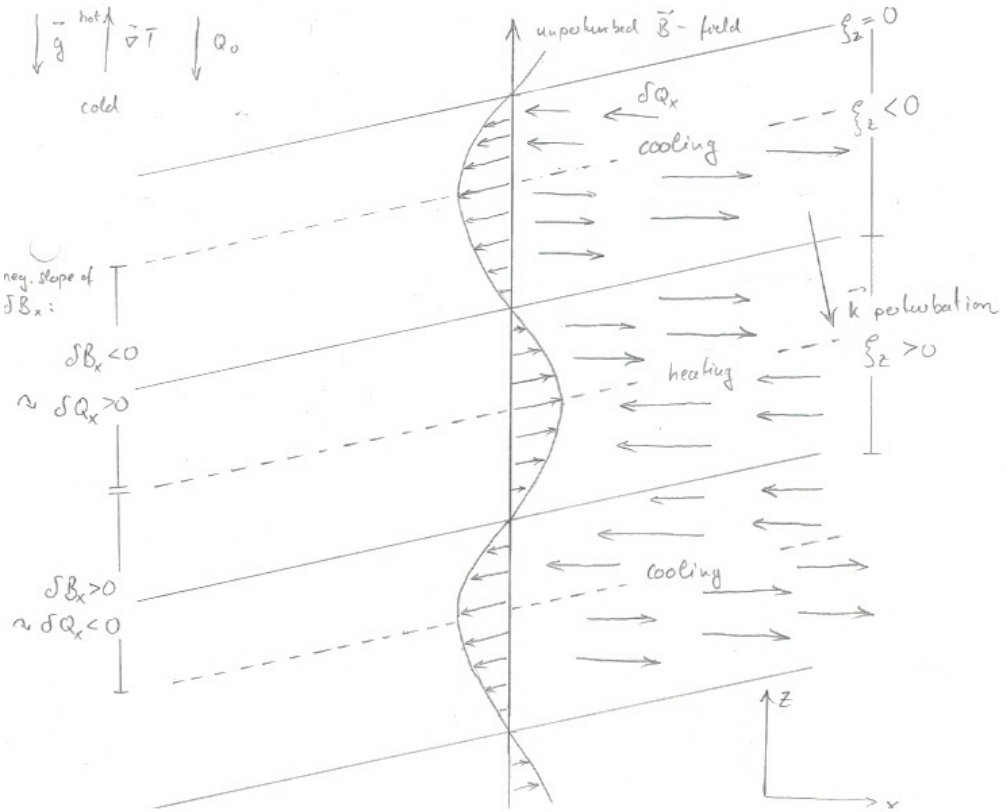

- The figure demonstrates that regions with a positive displacement field, $\xi_z > 0$, experience a converging perturbation of the heat flux, δQ_x which implies heating. This causes the upwards displaced fluid elements to rise further, which reinforces the perturbation and causes an instability.

Heat-flux driven buoyancy instability – 3

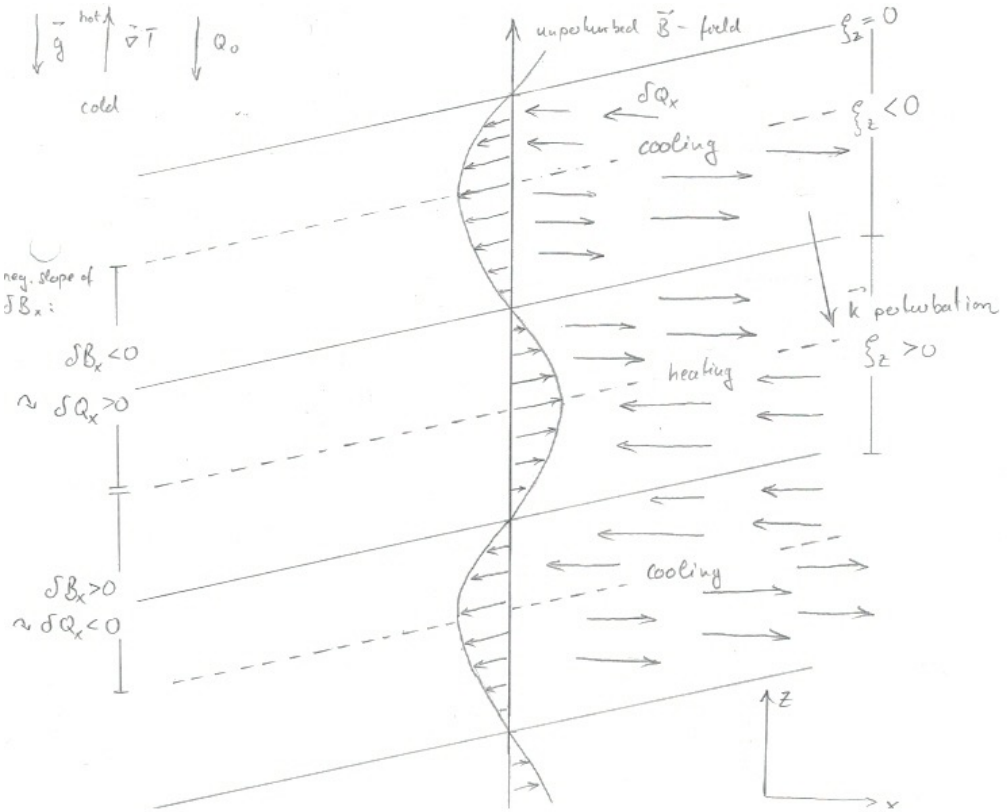

- The figure demonstrates that regions with a positive displacement field, $\xi_z > 0$, experience a converging perturbation of the heat flux, δQ_x which implies heating. This causes the upwards displaced fluid elements to rise further, which reinforces the perturbation and causes an instability.
- Equivalently, regions with $\xi_z < 0$ experience cooling. They become denser, heavier and continue to sink in the gravitational potential which reinforces the perturbation and causes an instability.

Heat-flux driven buoyancy instability – 4

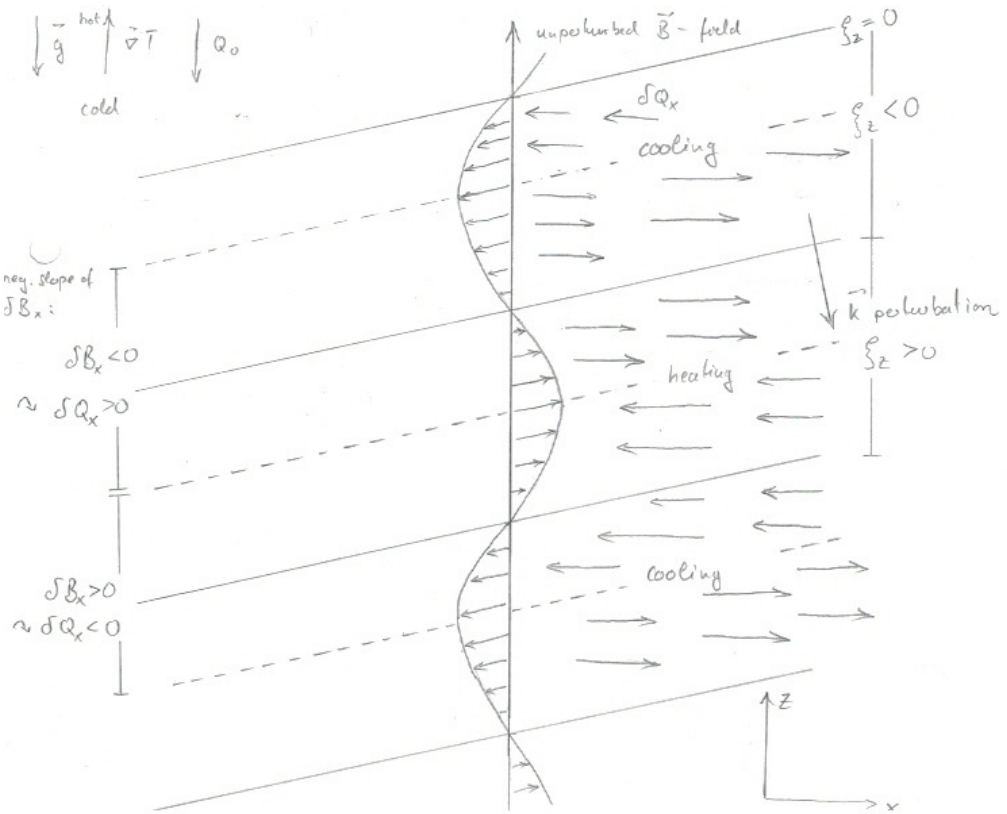

- Simulations of the non-linear stage of the instability demonstrate that the instability saturates quiescently with the magnetic field lines aligning horizontally (as suggested by the discussion of the linear regime of the instability), i.e., within the gravitational equipotential surfaces (shells of constant radius for a spherically symmetric cluster).

AIP

Heat-flux driven buoyancy instability – 4

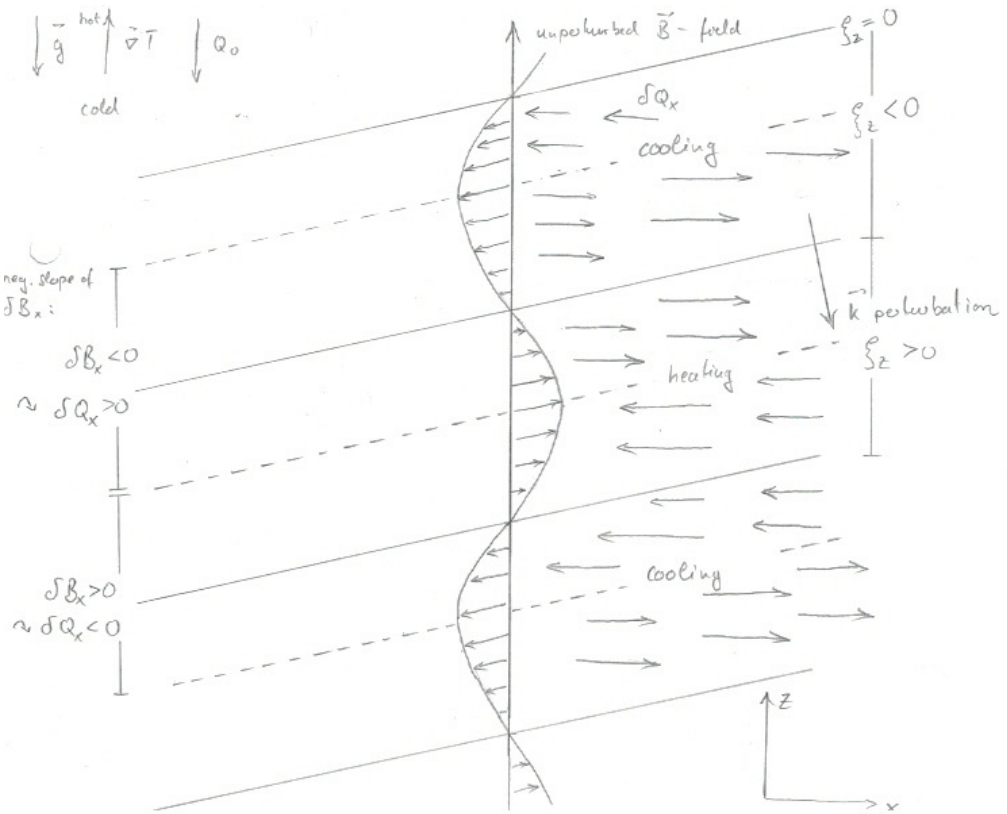

- Simulations of the non-linear stage of the instability demonstrate that the instability saturates quiescently with the magnetic field lines aligning horizontally (as suggested by the discussion of the linear regime of the instability), i.e., within the gravitational equipotential surfaces (shells of constant radius for a spherically symmetric cluster).

- This suppresses the inward heat flux by a large factor and thermally insulates the cooling core, which should reinforce the cooling catastrophe. Clearly, thermal conduction is not the solution to the cooling flow problem.

Heat-flux driven buoyancy instability – 4

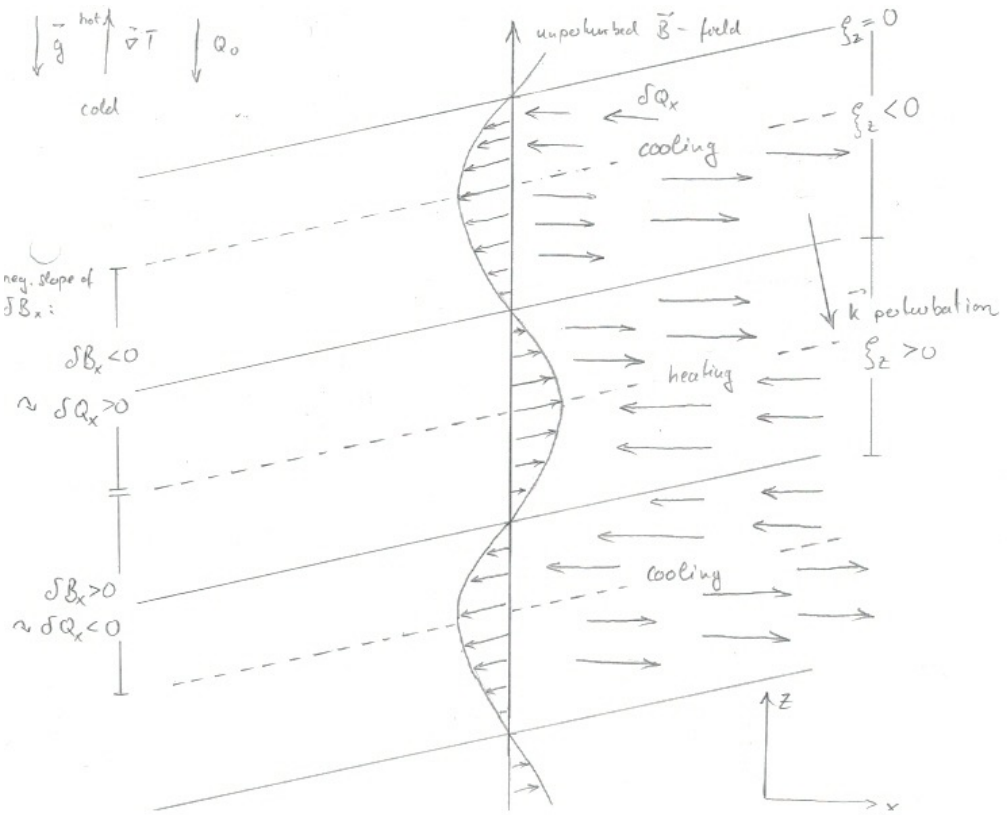

- Simulations of the non-linear stage of the instability demonstrate that the instability saturates quiescently with the magnetic field lines aligning horizontally (as suggested by the discussion of the linear regime of the instability), i.e., within the gravitational equipotential surfaces (shells of constant radius for a spherically symmetric cluster).

- This suppresses the inward heat flux by a large factor and thermally insulates the cooling core, which should reinforce the cooling catastrophe. Clearly, thermal conduction is not the solution to the cooling flow problem.
- The HBI is very vulnerable to external turbulence: only 1% turbulent pressure support in comparison to the thermal pressure is sufficient to isotropize the magnetic field and to quench the instability.

Heat-flux driven buoyancy instability – 5

- Do you have the heat-flux driven buoyancy instability (HBI) in a non-cool core (NCC) cluster?

Heat-flux driven buoyancy instability – 5

- Do you have the heat-flux driven buoyancy instability (HBI) in a non-cool core (NCC) cluster?
- No, because a NCC cluster has a constant central temperature profile and in order to trigger the HBI, you need an increasing temperature profile with radius.

Heat-flux driven buoyancy instability – 5

- Do you have the heat-flux driven buoyancy instability (HBI) in a non-cool core (NCC) cluster?
- No, because a NCC cluster has a constant central temperature profile and in order to trigger the HBI, you need an increasing temperature profile with radius.
- Do you always have the magneto-thermal instability in clusters? To this end, recap again our calculation of filling gas into an NFW potential.

Heat-flux driven buoyancy instability – 5

- Do you have the heat-flux driven buoyancy instability (HBI) in a non-cool core (NCC) cluster?
- No, because a NCC cluster has a constant central temperature profile and in order to trigger the HBI, you need an increasing temperature profile with radius.
- Do you always have the magneto-thermal instability in clusters? To this end, recap again our calculation of filling gas into an NFW potential.
- Yes, because if you had a profile of constant temperature in the outskirts, the gas density would decrease at a slower rate in comparison to the dark matter density so that the gas-to-dark matter fraction would exceed the universal baryon fraction, in contradiction with our cosmological concordance model.

AIP

- **Heat conduction:**
  * Collective action of small-angle scatterings is more important (by a factor of 70) in comparison to close-by large-angle scattering events
  * conductive heat flux scales $\propto T^{7/2}$: very important in hot, high-mass clusters

- **Heat conduction:**
  * Collective action of small-angle scatterings is more important (by a factor of 70) in comparison to close-by large-angle scattering events
  * conductive heat flux scales $\propto T^{7/2}$: very important in hot, high-mass clusters
- **Thermal instability – Field length:**
  * thermal instability only occurs on scales larger than the Field length λ_F below which thermal conduction smoothes out temperature inhomogeneities
  * if bremsstrahlung dominates gas cooling, then λ_F only depends on entropy
  * the gas of NCC clusters is always above the instability threshold, the gas in CC centers is thermally unstable so that conduction cannot balance cooling

- **Heat conduction:**
  * Collective action of small-angle scatterings is more important (by a factor of 70) in comparison to close-by large-angle scattering events
  * conductive heat flux scales $\propto T^{7/2}$: very important in hot, high-mass clusters
- **Thermal instability – Field length:**
  * thermal instability only occurs on scales larger than the Field length λ_F below which thermal conduction smoothes out temperature inhomogeneities
  * if bremsstrahlung dominates gas cooling, then λ_F only depends on entropy
  * the gas of NCC clusters is always above the instability threshold, the gas in CC centers is thermally unstable so that conduction cannot balance cooling
- **Thermal instability with magnetic fields:**
  * magnetic fields fundamentally change the convective stability criteria of weakly collisional plasmas such as the ICM
  * CC cluster centers are subject to the heat-flux driven buoyancy instability
  * the outskirts of all clusters are subject to the magneto-thermal instability